Durham Research Online

Deposited in DRO:

10 March 2017

Version of attached file:

Accepted Version

Peer-review status of attached file:

Peer-reviewed

Citation for published item:

Foulger, G.R. and Christiansen, R.L. and Anderson, D.L. (2015) 'The Yellowstone "hot spot" track results from migrating basin-range extension.', in The interdisciplinary earth : a volume in honor of Don L. Anderson. Boulder, Colorado: Geological Society of America, pp. 215-238. Geological Society of America Special papers. (514).

Further information on publisher's website:

http://specialpapers.gsapubs.org/content/514/215.abstract

Publisher's copyright statement:

Additional information:

Use policy

The full-text may be used and/or reproduced, and given to third parties in any format or medium, without prior permission or charge, for personal research or study, educational, or not-for-profit purposes provided that:

- a full bibliographic reference is made to the original source
- a link is made to the metadata record in DRO
- the full-text is not changed in any way

The full-text must not be sold in any format or medium without the formal permission of the copyright holders.

Please consult the full DRO policy for further details.

Durham University Library, Stockton Road, Durham DH1 3LY, United Kingdom
Tel : +44 (0)191 334 3042 | Fax : +44 (0)191 334 2971
https://dro.dur.ac.uk

The Yellowstone 'hot spot' track results from migrating basin range extension

G. R. Foulger[1], Robert L. Christiansen[2] & Don L. Anderson[3,§1]

[1]Dept. Earth Sciences, University of Durham, Durham DH1 3LE, U.K.,
g.r.foulger@durham.ac.uk

[2]U.S. Geological Survey, 345 Middlefield Road, Menlo Park, California 94025, USA,
rchris@usgs.gov

[3]California Institute of Technology, Seismological Laboratory 252-21, Pasadena, CA 91125,
dla@gps.caltech.edu

Abstract

Whether the volcanism of the Columbia River Plateau, Eastern Snake River Plain, and Yellowstone is related to a mantle plume or to plate tectonic processes is a long-standing controversy. There are many geological mismatches with the basic plume model as well as logical flaws, such as citing data postulated to require a deep-mantle origin in support of an 'upper-mantle plume' model. USArray has recently yielded abundant new seismological results, but despite this, seismic analyses have still not resolved the disparity of opinion. This suggests that seismology may be unable to resolve the plume question for Yellowstone, and perhaps elsewhere. USArray data have inspired many new models that relate Western USA volcanism to shallow mantle convection associated with subduction zone processes. Many of these models assume that the principal requirement for surface volcanism is melt in the mantle and that the lithosphere is essentially passive. In this paper we propose a pure plate model in which melt is commonplace in the mantle, and its inherent buoyancy is not what causes surface eruptions. Instead, it is extension of the lithosphere that permits melt to escape to the surface and eruptions to occur–the mere presence of underlying melt is not a sufficient condition. The time-progressive chain of rhyolitic calderas in the Eastern Snake River Plain-Yellowstone zone that has formed since basin-range extension began at ~ 17 Ma results from laterally migrating lithospheric extension and thinning that has permitted basaltic magma to rise from the upper mantle and melt the lower crust. We propose that this migration formed part of the systematic eastward migration of the axis of most intense basin-range extension. The bimodal rhyolite-basalt volcanism followed migration of the locus of most rapid extension, not vice versa. This model does not depend on seismology to test it but instead on surface geological observations.

[§] Deceased.

1 INTRODUCTION

Explaining how melt can exist in the mantle is not sufficient to explain surface volcanism. Melt is widespread in the shallow mantle and erupts where lithospheric extension permits it to do so. In the plate model, the lithosphere is the active agent that allows volcanism to occur. The lithosphere is not a passive, uninvolved interface between the mantle and the atmosphere through which melt passes transparently, as light passes through a sheet of glass. The mantle is not devoid of melt beneath regions where surface volcanism is absent. It is not required that melt formation and eruption to go hand-in-hand on the same timescale. In fact, the volumes and eruption rates in flood basalts preclude this (Cordery et al., 1997; Silver et al., 2006).

It is unlikely that a mantle-plume origin would ever have been suggested for the Eastern Snake River Plain-Yellowstone (ESRP-Y) zone were it not for the time-progressive chain of large rhyolitic caldera volcanoes there. The existence of such volcanic chains, and in particular their perceived fixity relative to the Hawaiian chain, was the cornerstone of the original plume hypothesis (Morgan, 1971). This hypothesis attributes relative fixity of volcanic loci on different plates to their sources being in the deep mantle, below the rapidly convecting shallow mantle associated with plate movements. This was required by the model because sources in rapidly convecting mantle were expected to move relative to one another. In the deep mantle, the only viable candidate source region for thermal plumes is the core-mantle thermal boundary layer.

Correcting the time-progression of the ESRP-Y rhyolitic volcanoes for the effect of basin-range lithospheric extension found that the relative fixity of the volcanic locus with respect to Hawaii was improved still further over uncorrected estimates (Rodgers et al., 1990). This has been taken to provide additional supporting evidence for a plume model for Yellowstone. Nevertheless, numerous seismological studies spanning nearly half a century essentially all agree that the seismic anomaly beneath the ESRP-Y zone is rooted in the shallow mantle (e.g., Burdick et al., 2012; Christiansen et al., 2002; Courtillot et al., 2003; Iyer et al., 1981a; James et al., 2011; Montelli et al., 2006; Montelli et al., 2004a; Montelli et al., 2004b; Ritsema and Allen, 2003; Schmandt and Humphreys, 2010; Tian et al., 2009; Xue and Allen, 2010). Estimates for the bottoming depth range from 200 km to a maximum of 1000 km. These studies include numerous sophisticated recent studies conducted by multiple research groups using data from USArray. This array comprises a 2000-station network spanning the entire contiguous 48 states, and has an areal extent of ca. 8000 x 2250 km. The data it returned are unprecedented in quality, quantity, and breadth of the monitoring area, and are unlikely to be surpassed in the near future.

A shallow provenance for mantle processes associated with ESRP-Y volcanism immediately weakens the argument that the time-progressive volcanic chain supports a mantle plume interpretation. The fundamental premise of the hypothesis was that deep origins, below the shallow, rapidly convecting layer, were required to explain relative fixity of the volcanic loci. The plume hypothesis cannot explain relative fixity of volcanic loci fed from the shallow mantle, in particular in structurally and dynamically complex parts of the mantle such as that beneath the W USA. It is not clear why a long-lived, thermally buoyant upwelling fixed relative to Hawaii should spontaneously arise in the upper mantle nor how it could be sustained. A second argument frequently cited as conclusive evidence for a plume–the observation of high $^3He/^4He$ isotope ratios–is, as a consequence, also suspect. This is because the theory that such isotope ratios indicate plumes rests on arguments that only the core-mantle boundary region has sufficiently high $^3He/^4He$ to be the source.

These observations imply that the time progression of rhyolitic volcanism and its associated upper-mantle magmatism in the ESRP-Y zone are not induced by a plume arising from the base of the mantle. If so, some other process must be responsible. The Janus twin of the ESRP-Y zone, the mirror-image, east-to-west-migrating High Lava Plains time-progressive volcanic chain (the 'Newberry trend'), has been attributed to interaction of the lithosphere and evolving shallow mantle convection associated with the subduction zone to the west. If such processes can explain the time-progression of the Newberry trend, it follows that they might also explain that of the ESRP-Y zone.

This paper summarizes briefly some of the now extensive body of seismological information on the mantle beneath the W USA in the neighborhood of the ESRP and Yellowstone. Current plume- and plate-related models are reviewed. We propose a new, pure plate model for the ESRP-Y zone. In this model, volcanism is permitted by an evolving, migrating pattern of lithospheric deformation. We do not assume that the planform of surface volcanism merely reflects melt-existence in the mantle, with little influence from a passive lithosphere. Our model for ESRP-Y volcanism is based on surface observations. It does not appeal to non-unique interpretations of remotely sensed mantle seismic structure. Instead, it is tractable for testing using surface geological observations.

2 FRAMEWORK

The basalts of the Columbia River Plateau (the CRB) and the ESRP-Y volcanic provinces together (Figure 1) are regarded by many as the products of the type example continental mantle plume. It has been argued that these provinces are consistent with an initial plume head forming a flood basalt, followed by a time-progressive volcanic trail leading to a currently active volcanic locus. This comprises one of only three cases in the world where time-progressive volcanism is spatially associated with a flood basalt of the appropriate age (Courtillot et al., 2003).

Despite this, many aspects of the region do not fit this model (e.g., Christiansen, 2001; Christiansen et al., 2002):

1. The uplift claimed to have heralded plume-head arrival is based on ambiguous observations that could equally well be interpreted as indicating climate change (Bull, 1991; Foulger, 2010, p 50; Hooper et al., 2007). Any uplift was local. Regional vertical motions were studied by Hales *et al.* (2005) who reconstructed the presumed-initially flat topography of individual lava flows. This work found that regional subsidence, not uplift, preceded CRB eruption (Hales et al., 2005; Humphreys et al., 2000; Sheth, 2007);
2. Almost all of the 234,000-km^3, 1.8-km-thick CRB erupted very quickly, over ~ 1.6 Ma (Pierce and Morgan, 2009). This is much faster than the 10 - 20 Ma predicted by numerical modeling of arriving plume heads (Farnetani and Richards, 1994);
3. The flood basalt lavas erupted from parts of a relatively narrow ~ 900-km-long zone of fissures that lie along the late Precambrian rift margin of North America (Figure 1). This is more consistent with a linear source than a point source. The ~ 300 x 600-km, roughly oval flood basalt does not reflect the geometry of the magma source, but the topography of the land at the time of eruption (Christiansen et al., 2002);
4. The geochemistry of the CRB corresponds to shallow adiabatic decompression melting of mantle lithosphere, and the depths and temperatures of melting correspond to ~100 km and normal mantle temperatures near the base of the crust (e.g., Long et al., 2012).

The composition of CRB is different from basalts of the ESRP-Y zone, most notably in TiO_2, P_2O_5, SiO_2 and alkalis. There is, thus, no geochemical evidence that they come from the same source;

5. The oldest end of the ESRP-Y zone, the McDermitt Caldera, lies south of the Steens Mountain and other main CRB eruptive fissures, and 400 km south of the largest eruptive centers (Camp, 2013; Pierce et al., 2002). This is not consistent with ESRP volcanism being fed by a CRB 'plume tail', which would necessitate a migration rate up to 6.2 cm/yr from 17 - 10 Ma, much faster than the 2.5 cm/yr that occurred between later volcanoes (Anders, 1994);
6. The volcanism that began at ~16.1 Ma with formation of the McDermitt caldera was not an isolated event but part of major tectonic reorganization throughout much of a region 2,000 km wide that included the newly forming, volcanically productive, basin-range region (Christiansen and Lipman, 1972; Christiansen and McKee, 1978). This onset of northeastward-propagating volcanism occurred at the western edge of the Archean North American craton (Hoffman, 1989);
7. McQuarrie and Rodgers (1998) report that more than half of the total subsidence of the ESRP occurred before eruption of a 6.6-Ma ignimbrite from the major caldera center just west of Yellowstone. This indicates that downwarping preceded this portion of the time-progressive rhyolitic volcanism, the opposite of what is expected for 'plume tail' volcanism;
8. The ESRP-Y volcanic zone existed in some form prior to the arrival of major caldera-forming eruptions. For example, smaller silicic eruptions occurred as early as ~ 10 Ma a few tens of kilometers south of Yellowstone and elsewhere in the northern Basin Range province, well before major caldera-forming volcanism (Christiansen and McKee, 1978; Christiansen and Yeats, 1992; Love, 1956; Love et al., 1973) ;
9. The distribution of ESRP rhyolitic volcanism between 10.2 and 2 Ma was not a simple linear time progression. Rather, volcanism developed large caldera systems that evolved in place, gradually extinguished, then initiated in a new location in stepwise progression (Christiansen, 2001; Pierce and Morgan, 2009);
10. The calderas are blanketed and buried by post-caldera tholeiitic basalt which erupted continuously for hundreds of kilometers along the ESRP without spatial migration. This basaltic volcanism, which has been continuous to the present, is not predicted by the plume hypothesis (Campbell, 2007);
11. There is no evidence in the form of high-temperature petrologies, *e.g.*, picrite glass or komatiite-like magmas, for the high melt-source temperatures expected for a mantle plume 200-300˚C hotter than the regional mantle (Davies, 1999; Foulger, 2012, Ch. 6);
12. Simultaneous with northeastward migration of volcanism along the ESRP-Y zone, volcanism also migrated northwestward across the High Lava Plains (the "Newberry trend") (MacLeod et al., 1976). These paired volcanic chains do not lie at random places but run along the northern margin of basin-range extension;
13. To the south of the ESRP-Y zone, the basin-range region has widened by ~250 km since volcanism began at ~ 17 Ma (Wernicke and Snow, 1998). To the immediate north however, extension has been no more than a few tens of kilometers, dwindling within a few tens of kilometers farther northward to essentially zero (Christiansen and McKee, 1978; Christiansen and Yeats, 1992; Lawrence, 1976);
14. The ESRP-Y zone, functioning essentially as a transfer zone between regions of differential extension (Christiansen and McKee, 1978; Christiansen and Yeats, 1992; Payne et al., 2008), lies at a profound change in lithospheric structure between thin, hot, extending lithosphere to the south and thick, cold lithosphere underlying the North American craton to the north. This zone is also marked by a regional aeromagnetic

anomaly that runs along the axis of the ESRP from Nevada, northeastward through Montana and on to Canada (Eaton et al., 1975; Mabey et al., 1978);

15. Numerous Precambrian geologic and geophysical alignments that parallel the ESRP-Y zone suggest deep-seated lithospheric structural control. O'Neill and Lopez (1985) identified a complex broad zone of diverse northeast-trending features, the Great Falls tectonic zone. This zone is at least 250 km wide and 600 km long and lies north of the ESRP-Y, crossing younger Rocky Mountains structural trends. Thomas *et al.* (1987) and Hoffman (1989) regarded it as the expression of a Paleoproterozoic suture between the Archean Wyoming and Hearne provinces though Boerner *et al.* (1998) consider it an intracontinental shear zone. The Madison mylonite zone (Erslev, 1983) lies along its southeastern exposed margin. Deep-seated structures detected by seismic and potential-field surveys demonstrate the lithospheric scale of both the Great Falls tectonic zone and the Archean Wyoming province (Lemieux et al., 2000);
16. Other magmatic zones in the basin-range region are also oriented parallel to the ESRP-Y zone, in particular, the Valles and the St. George zones (Smith and Luedke, 1984). These zones also parallel regional lithospheric structures of Precambrian origin (Ander et al., 1984; Dueker et al., 2001; Humphreys and Dueker, 1994; Karlstrom et al., 2002). They too have erupted both rhyolite and basalt over the same time period as the ESRP-Y zone although their volcanism is not time-progressive. Nevertheless, the seismic structure beneath them is similar to that of the ESRP-Y province. Beneath the Valles zone, low velocities in the mantle extend to even greater depths than beneath the ESRP-Y zone (Section 3.4) (Burdick et al., 2012).

As a consequence of the above observations, opinion regarding the origin of CRB-ESRP-Y volcanism varies widely. Since USArray data have become available, many studies have attempted to resolve the question and the ESRP-Y region has become the most intensively studied melting anomaly in the world. These studies have returned varied results but have not produced reliable, repeatable evidence for a plume. Nevertheless, opinion still remains divided (e.g., Christiansen et al., 2002; Tian and Zhao, 2012). Briefly reviewing some of these seismological studies is the task of Section 3 of this paper.

In the light of many new seismic tomography images a wide range of new models has been proposed for CRB-ESRP-Y volcanism. Any successful model in addition has to explain in particular the NS-oriented, 900-km-long array of CRB and other contemporaneous eruptive fissures, the two oppositely-propagating time-progressive chains of rhyolitic central volcanoes, and the widespread basaltic volcanism and basin range extension throughout an ~ 800-km-wide province. Models proposed previously fall into three broad classes:

1. A mantle plume;
2. Upper-mantle-convection related to subduction-zone evolution (assuming the lithosphere to be passive); and
3. Upper-mantle-convection combined with lithospheric extension, assuming the lithosphere to influence the site of volcanism, but not the fundamental fact that it occurs.

None of these are pure 'plate' models that view the lithosphere as the active element (Foulger, 2010). The plate hypothesis proposes that volcanism results from lithospheric extension, driven by plate-tectonic processes, that permits the escape of melt to the surface. The volume erupted is dependent on the amount available in the mantle which is, in turn, dependent on many processes, including convection. However, the mere presence of melt in the mantle *per se* is not a sufficient explanation for surface eruptions.

Therefore, in this paper we thus propose a fourth class, a pure plate model, for the ESRP-Y zone:

4. Lithospheric extension driven by plate-boundary processes, that allows pre-existing melt to erupt.

3 SEISMIC STRUCTURE OF THE MANTLE

Of all major melting anomalies on Earth, the ESRP-Y region is the best placed for study using seismology because of its position within the north American continent. Consequently it is the most comprehensively studied. It has been the target of several ambitious seismometer deployments and the full suite of seismic methods has been applied, including diverse tomography approaches and study of the transition zone (TZ) using receiver functions. Seismic tomography (a term first proposed by Anderson and Dziewonski (1984)) has been conducted on local, regional, and whole-mantle scales and, most recently, on a continental scale using data from the ~ 2000-station USArray network that covered the entire country over the period 2004 - present (http://www.usarray.org).

3.1 Caveats On Seismic Tomography

The results of tomographic experiments can vary considerably according to the data-inversion- and plotting strategies used (Foulger et al., 2013). The values chosen for factors such as damping may be fairly arbitrary, within bounds, but can have a major effect. A strongly damped inversion will produce relatively simple models with broad, weak anomalies whereas a weakly damped inversion will produce more complex models with smaller, stronger anomalies. There is no fully objective method for choosing the correct damping factor, and in general amplitudes of anomalies are probably underestimated by a factor of several (Sun and Helmberger, 2011). The effect of structure outside the study volume on the approach directions of rays is ignored in many inversion methods. This means that the seismic rays used do not necessarily travel along the paths assumed. This will have an unknown corrupting effect on the results.

A particular problem for the ESRP-Y region is that of inhomogeneous ray coverage. Because the dominant source of recorded earthquakes is the circum-Pacific belt, a large majority of rays approach at angles of ~ 20-30° to the vertical, from NW or SE azimuths. This will produce preferred smearing of anomalies along those incoming ray directions. Such smearing is visible in all teleseismic tomography images of the region.

Despite widespread assumptions, teleseismic tomography does not yield the three-dimensional structure of the study volume but only lateral variations in structure in each independent layer (Foulger et al., 2013 Section 2.3). Apparent continuity of imaged anomalies between the layers is controlled by the assumed 'normal' background seismic velocity for each layer. Neglect of anisotropy will work to create low-velocity artifacts in regions where melt lamellae exist (Anderson, 2011). Checkerboard tests do not have the power to determine which, if any, parts of a study volume have been imaged reliably because they do not test resolving power for the real structure present. A non-technical summary of these problems is presented by Foulger *et al.* (2013).

In addition to these challenges, there is a wide choice of approaches to displaying the results, including choice of color scale, use of smoothing and interpolation to produce images that look ‘natural’, and selection of lines of section that yield images that fit best the preferred model. Assessment of the results may be out of reach for non-seismologists as a practical matter because errors are rarely published in a way that is straightforward to deal with, models may not be available on the internet, plotting tools provided may be challenging to use and the outputs non-uniform in appearance (Pavlis et al., 2012).

Most problematic, perhaps, is the fact that interpretation of anomalies is ambiguous. The effects of lithology, melt content and temperature cannot be unambiguously separated out. Seismology cannot be used as a thermometer, and seismic velocity anomalies cannot be interpreted solely as temperature variations. Even if the different effects could be known, because amplitudes cannot be reliably determined, strengths of the anomalies cannot be reliably interpreted.

Given these issues, it is an unsurprising if inconvenient fact that there is limited repeatability among the many tomographic results available, including those recently produced using USArray data (Section 3.4). Furthermore, there is a diverse range of interpretations.

3.2 Early studies–teleseismic tomography

Teleseismic tomography to study the mantle beneath Yellowstone was pioneered in the 1970s by Iyer *et al.* (1981b) who deployed a 57-station network of vertical short-period seismometers over an area of 430 x 250 km. That experiment detected a low-V_P anomaly in the upper crust, decreasing in strength in the lower crust and upper mantle. Christiansen *et al.* (2002) reprocessed the data, finding strengths of typically –4-5% throughout the main low-V_P body (Figure 2). They confirmed the results of Iyer *et al.* (1981b), that the anomaly terminates at ~ 200 km depth, ruling out deeper bodies with V_P anomalies stronger than about –1% and dimensions comparable to the shallower anomaly. At greater depth, immediately beneath Yellowstone, high-V_P was imaged at 300-400 km.

Additional weak anomalies, both high- and low-V_P, tilting at ~ 20-30° to the vertical to both the NW and SE, were also imaged by Christiansen *et al.* (2002). These anomalies extend down to ~400 km. Doubt was cast on their veracity because they are weak and parallel to bundles of incoming rays. They were critically examined using resolution analysis, and it was concluded that they are artifacts resulting from smearing of the strong, shallow body along the ray bundles. Christiansen *et al.* (2002) concluded that the strong, shallow, low-V_P body does not extend deeper than the sub-lithospheric low-velocity zone, which has its base at ~ 200 km depth. The strong, shallow low-V_P body is continuous to the west-southwest beneath the ESRP in the depth interval ~50-200 km, but not elsewhere.

Later work using networks of modern, digital, three-component seismometers yielded similar results. Yuan and Dueker (2005) imaged a strong, low-V_P anomaly in the upper ~ 250 km beneath the ESRP-Y zone and high-V_P anomalies at greater depth beneath Yellowstone (Figure 3). They found the strength of most of the low-V_P anomaly to be ~ 1.5%, reaching a maximum of ~ 3.2%. Like Christiansen *et al.* (2002), they also imaged deeper anomalies, both high- and low-V_P, tilting down and away from Yellowstone (Figure 3).

The existence of the strong, shallow, low-V_P anomaly is not in dispute. However, it is on the significance and interpretation of the weaker, deeper low-V_P anomalies that the debate rests regarding the depth of origin of ESRP-Y volcanism. In the images presented by Yuan and Dueker (2005), one of these deep anomalies, tilting to the NW, is continuous with the shallow anomaly and extends to ~ 500 km depth (Figure 3). This deeper anomaly has a strength of ~ 0.5% throughout most of its volume, reaching a maximum of ~ 0.9%. Yuan and Dueker (2005) interpreted it as a plume tail. The same feature, detected by Christiansen *et al.* (2002) (Figure 2), was considered to be discontinuous, and an artifact due to smearing along an incoming ray bundle.

The amplitudes of the anomalies imaged in the two inversions differ significantly. Christiansen *et al.* (2002) reported strengths of up to ~ 4-5% and a compact body, and Yuan and Dueker (2005) strengths of up to ~ 3.5% and a more distributed body.

3.3 Whole-mantle tomography

The minimum size of bodies that can be resolved by whole-mantle tomography is at the level of hundreds of kilometers where station coverage is good and teleseismic earthquakes plentifully recorded. This increases to a thousand kilometers or more where conditions are poor, which is insufficient to detect bodies only a few tens of kilometers in diameter (Hwang et al., 2011). Nevertheless, a review would not be complete without brief mention of these results.

No hint of a mantle plume beneath Yellowstone has been found in whole-mantle tomography (Figure 4) (e.g., Montelli et al., 2006; Montelli et al., 2004a; Montelli et al., 2004b; Ritsema et al., 1999). Whole-mantle images do, however, serve well to emphasize the profundity of the lithospheric structural change at Yellowstone. There, low seismic velocities beneath the Basin and Range province to the southwest are juxtaposed against the high-velocity, thick lithosphere of the north American craton to the northeast. Despite the difference in scale of bodies resolvable, the structure observed in the whole-mantle cross section shown in Figure 4 corresponds in some detail to what is observed using teleseismic tomography, with high velocities being detected beneath the low velocities in the shallow mantle beneath Yellowstone (Figure 2).

3.4 Continental-scale tomography using USArray data

Since inception of the USArray project in 2004 a vast database of seismic recordings has accumulated which has been used by numerous research groups to study the structure of the mantle beneath the contiguous 48 states (Burdick et al., 2012; James et al., 2011; Obrebski et al., 2010; Schmandt and Humphreys, 2010; Tian et al., 2009; Tian and Zhao, 2012; e.g., Xue and Allen, 2010). Beginning with the installation of ~ 400 stations in a swath covering Washington, Oregon and California, USArray migrated progressively east and has now almost completed its sweep across the continent. The unprecedented size of the area covered has yielded tomographic images with higher resolution to greater depths in the mantle than has been achieved before.

Many images and several models of the mantle beneath the W USA have now been published, some on the internet, and several with particular focus on the ESRP-Y region. Many of the same issues affect these results as confuse the results of teleseismic tomography (Section 3.1). These include damping-related variations in the complexity of the results, in particular the anomaly strengths between models (Becker, 2012). Other problems include inhomogeneous ray distribution, variations in background model used, variations in model parameterization and inversion techniques, and likely corruption of results from unmodeled structure outside the study region. Checkerboard tests are routinely used to claim significance for imaged features despite the fact that the same features may not be seen in other models that are supported by other checkerboard tests. Repeatability is achieved only for the largest, strongest, first-order features. For second-order, small-scale and weak features, including the detailed shape and strength of the larger features, repeatability is low.

A useful contribution to understanding the bewildering suite of results was made by Pavlis *et al.* (2012). They compared 12 mantle models produced using USArray data, including nine body-wave tomography models, one surface-wave tomography model, one model obtained using both surface and body waves and one three-dimensional wavefield image. This involved resampling the data and rendering them to a standard format so that each could be visualized using a single open-source visualization software package. The data were made available by the original authors in different formats, and some had not been published along with the original papers. Assembling these data for comparison purposes was a significant task and illustrates the practical difficulties that face cross-disciplinary researchers wishing to use the seismic-tomography results obtained by others.

Some of the main features revealed by studies using USArray data include:

1. Relative to the region east of the Rocky Mountains, the W USA is associated with widespread low velocities that are strongest in the upper ~ 300 km. These low velocities are particularly prominent beneath the California coastal ranges, the Sierra Nevada, the Basin and Range province, Arizona, and New Mexico, with tongues of low velocity underlying the ESRP-Y zone, the Valles zone and the St. George zone (Figure 5). At greater depth, velocities are lowest beneath Arizona. Anomalies weaken at TZ depths;
2. The subducting Farallon slab bottoms at TZ depths or a little below under the W USA. It is fragmented and has a gap or tear beneath E Oregon (Pavlis et al., 2012). It is unclear where the ~ 5,000 km of oceanic lithosphere subducted since the Cretaceous lies (Schmandt and Humphreys, 2010; Tian et al., 2009);
3. The ESRP-Y region is underlain by shallow, ultra-low seismic velocities in the upper 200 km. This anomaly is one of the strongest low-velocity features observed anywhere in the continental lithosphere;
4. Velocity anomalies at depths > 200 km beneath Yellowstone have received particular attention. All studies find them to be weak, and between studies there is considerable variation in detail. Xue and Allen (2010) report a low-velocity anomaly that dips to the NW, bottoms at 500 km depth, and is seen in V_P but not V_S. They rule out a deeper body wider than 50 km and stronger than –1.5% in V_S and –0.75% in V_P. In a paper published just nine days later, the same group report an inversion showing a continuous, corkscrew-shaped 'whole-mantle plume' bottoming at 900 km depth in both V_P and V_S (Obrebski et al., 2010). They report good recovery of structure down to 1200 km depth. Tian and Zhao (2012) image low velocities under Yellowstone extending to at least 1,000 km. Schmandt and Humphreys (2010) report discontinuous low-velocity anomalies and find no evidence that they extend into the lower mantle. James *et al.* (2011) image a convoluted sub-vertical sheet of low-velocity material extending the entire length of the ESRP-Y zone. Adams and Humphreys (2010) invert for upper mantle attenuation and interpret the results jointly with velocity tomography. They conclude that the strong anomaly in the top ~ 200 km is less attenuative than the adjacent mantle, a counter-intuitive result. Tian *et al.* (2009) report an imbricated, discontinuous pair of low-velocity bodies, one terminating at 500 km depth and the other extending to 1000 km depth;

5. Most studies report high velocities in the TZ beneath the Yellowstone region (Becker, 2012; Pavlis et al., 2012).

Figure 6 shows cross sections through nine of the models studied by Pavlis *et al.* (2012). The sections run from Cape Mendocino, through the NW basin-range province, along the ESRP and on into the north American craton. The repeatable features and variations between models are immediately clear. Only the largest, strongest, first-order features are common to most images. These are, from W to E, the subducting, high-velocity Farallon slab, the strong low-velocity anomaly underlying the length of the ESRP down to a depth of ~ 200 km, and the high-velocity N American craton in the E. Both high- and low-velocity anomalies become less repeatable between models with increasing depth. Low-velocity anomalies at depths > 200 km beneath the Yellowstone region are weaker than the shallower anomalies, with poor repeatability between models (Foulger et al., 1995; Foulger et al., 2013).

3.5 The transition zone

The TZ discontinuities at 410- and 660 km are thought to result largely from mineral-phase transitions in the peridotite mantle. Their exact depths are affected by pressure, temperature, and composition, including water. High temperatures, dry conditions and high-Mg content are thought to deepen the 410-km discontinuity and shallow the 660-km discontinuity, thus thinning the TZ (Bina and Helffrich, 1994; Ghosh et al., 2013; Katsura et al., 2004; Presnall, 1995; Wood, 1995). The behavior of the two discontinuities is expected to be anticorrelated because of the opposite signs of the Clapeyron slopes of their respective olivine mineral-phase changes. Multiple phase changes occur at about 660 km depth, and this complication renders the behavior of that discontinuity less certain (Vacher et al., 1998).

TZ discontinuity topography has been measured using the receiver-function technique. Early work assumed simplistically that three-dimensional velocity variations could be neglected and that topography was controlled only by temperature. The method was therefore commonly used as a thermometer. It was extensively applied in purported plume localities where the task at hand was commonly to identify the place where the TZ appeared to be thinnest and to propose this as the TZ-crossing place of the assumed hot plume. Offsets from the surface location of most intense volcanism were explained as tilting plumes (e.g., Shen et al., 2002), mantle wind (e.g., Steinberger et al., 2004), or disruption of the assumed plume conduit by upper-mantle structural complications (e.g., Fee and Dueker, 2004).

The receiver-function technique has been used in the Yellowstone region in several studies, which have yielded varied results. Dueker and Sheehan (1997) and Fee and Dueker (2004) used pre-USArray data from several experiments and found uncorrelated TZ discontinuity topography on the 410- and 660-km discontinuities of ± 35-40 km. They found a depression in the 410-km discontinuity of ~ 18 km centered ~ 130 km NNW of Yellowstone, with a flat 660-km discontinuity beneath. This locality coincided with the weak, downward extension of the shallow low-V_P body reported by Yuan and Dueker (2005). Fee and Dueker (2004) concluded that the region of deepened 410-km discontinuity corresponds to a ~ 200˚C temperature anomaly, with no temperature anomaly at 660 km. They also found a ~ 20-km shallowing of the 660-km discontinuity ~ 400 km NE of Yellowstone, where the 410-km discontinuity also shallows by ~ 15 km. Interpreted in the same way, this would suggest a temperature anomaly of ~ + 200˚C at 660-km depth and -200˚C at 410-km depth. Neither discontinuity was reported to be significantly perturbed under an adjacent area where V_P is high. The uncorrelated ± 35-40 km topography on the discontinuities would require ~ 400˚C variations in temperature anomalies, apparently uncorrelated with surface features. Such interpretations are implausible.

Beucler *et al.* (1999) re-analyzed the same data using different techniques and obtained very different results. They found the 410-km discontinuity to have a fragmented aspect that precluded accurate mapping of TZ thickness, and the 660-km discontinuity to be strongly deflected. They concluded that the TZ was complicated by Farallon slab fragments and that no evidence could be found in support of a TZ-penetrating hot body as suggested by Dueker and Sheehan (1997) and Fee and Dueker (2004). Beucler *et al.* (1999) further suggested that, in addition to temperature, composition and volatile content, TZ-discontinuity depths can also be affected by the kinetic effects of actively subducting slabs.

Later work reported still different results. Schmandt *et al.* (2012) utilized USArray data to study the TZ and found it to be ~ 4 km thicker than the global average throughout the entire W USA. This finding is inconsistent with temperature-related interpretations of TZ thickness in view of the magmatically active nature of the region. In the Yellowstone region they found very different results from those of Fee and Dueker (2004). They report that the 660-km discontinuity is 12-18 km shallower than normal (with a 2σ error of 16.6 km) beneath a large area centered 75 km northeast of Yellowstone, but that the 410-km discontinuity was at normal depth everywhere in the vicinity. They interpreted their results to propose a TZ-crossing hot plume that is disrupted by mantle structural heterogeneity above 660 km. Implausibly high estimated temperatures of ~ 700˚C led them to attribute some of the topography of the 660-km discontinuity to non-thermal effects such as anhydrous mineralogy.

Most recently Gao and Liu (2013) introduced a new method to deal with the problem of trade-offs between the discontinuity depths and velocity heterogeneity above. They used both converted and multiply reflected phases, and *P*-to-*S* converted phases, to simultaneously determine the discontinuity depths and velocity anomalies. They applied the method to a NS swathe 780 km long and 336 km wide centered on Yellowstone. Low velocities were detected, but no significant topography on either the 410- or 660-km discontinuities.

3.6 Interpretation of the seismic results

What can be concluded from these results regarding Yellowstone? It is a robust result that ultra-low seismic velocities underlie the ESRP-Y in the upper 200 km along its entire length. The nature of low-velocity anomalies at greater depth is controversial, however. No coherent low-velocity anomaly is repeatably imaged that extends continuously from the surface down into the lower mantle. High-velocity bodies littering the TZ under the ESRP-Y zone, interpreted as fragments of the Farallon slab, make a through-going plume more implausible. Figure 6 serves well to illustrate the variability between models. Below 200 km depth, low-velocity regions imaged vary from large, rounded blobs several hundred kilometers in diameter, to weak, fragmented, vertically elongated features. Equally strong low-velocity anomalies are widespread beneath other regions (Figure 5).

The weak, low-velocity anomalies that are imaged below ~ 200 km have been interpreted both as artifacts of smearing of the shallow anomaly along incoming ray bundles and as a real and continuous extension of the shallow anomaly. Neither interpretation suggests a deep mantle plume. Thermal interpretations are non-unique and find little support in the suite of studies of TZ discontinuity topography which, like seismic tomography, yields poor repeatability.

Under these circumstances, interpretations may be influenced by authors' model preferences. Several authors interpret low-velocity bodies as hot plumes, including both downward-continuous and fragmented types, and ones confined to the upper mantle. Xue and Allen (2010) base their interpretation on the assumption that the gap in the Farallon slab must have been caused by an arriving Yellowstone plume head. Despite not imaging an anomaly in the lower mantle, they cite the time-progressive chain of rhyolitic volcanoes on the ESRP, high-$^3He/^4He$, and a CRB magma source containing recycled oceanic crust, as evidence in support of a plume. They attribute the time-progressive Newberry volcanic chain to upper-mantle processes. Obrebski *et al.* (2010) interpret the low-velocity anomaly beneath the ESRP as part of a plume head, whereas Tian and Zhao (2012) attribute it to hydrated minerals. Obrebski *et al.* (2010) suggest a Yellowstone plume rose opportunistically through a pre-existing tear in the downgoing Farallon slab. James *et al.* (2011) interpret the sheet-like low-velocity body they image as evidence that CRB and ESRP-Y volcanism arose from poloidal and toroidal upwellings around the edges of a fragmented subducted Farallon plate. Adams and Humphreys (2010) attribute to dehydration their finding that the strong anomaly in the top ~ 200 km under Yellowstone is less attenuative than the adjacent mantle. They estimate a temperature anomaly of 30-50˚C for the deeper part of the anomaly, with higher temperatures at shallower depth.

4 MODELS FOR EASTERN SNAKE RIVER PLAIN-YELLOWSTONE VOLCANISM

All continental-scale seismic tomography images for the W USA show a complex mantle. Interpretations have associated these complexities with the collage of major tectonic features that make up the W USA including the fragmented, subducted Farallon slab, the delaminated Sierra Nevada, the basin-range region, the ESRP-Y, the Valles zone and the St. George zone. Many models seek to account for W USA volcanism by explaining how melt can form in the mantle beneath. Many models consider the fragmented state of the Farallon slab to be pivotal. A minority of models interpret the observations essentially solely in terms of a simple subducting slab disrupting an independent deep mantle plume.

Explanations for W USA magmatism linked to retreat of the subduction hinge and lithospheric extension were suggested as far back as the 1970s (e.g., Cross and Pilger, 1978). Ford *et al.* (2012) attribute the age-progressive Newberry trend to mantle upwelling in response to slab rollback. This explanation does not, however, explain why the age-progressive volcanism should comprise a narrow zone and not a broad region, nor does it explain the decoupling between the rhyolitic and basaltic volcanism along that trend.

Faccenna *et al.* (2010) suggest that small-scale convection brought about by Farallon slab dynamics and return flow results in focused upwellings in which melt forms via decompression. They envisage upper-mantle upwellings occurring in general in areas that are floored by subducted slab in the TZ, with melt formed near its end and edges, in the back-arc area, and in response to slab retreat and tearing. Changes in relative trench motion and subduction velocity can introduce further complexities. They argue that such upwellings would produce temperature anomalies at the surface, transport H_2O which would encourage melting, and that the petrologies predicted are supported by observations. They draw a comparison with European volcanism, which occurs behind the Mediterranean subduction zone. In common with other models, Faccenna *et al.* (2010) seek to explain surface volcanism solely by the formation of melt in the mantle, with the lithosphere viewed as an essentially non-participative interface separating the mantle and the atmosphere.

Liu and Stegman (2012) attribute the CRB to an episode of tearing in the Farallon slab that permitted upwelling of sub-slab asthenosphere, decompression and melting. The rupture is proposed to have started under E Oregon at ~ 17 Ma and to have propagated north and south to attain a length of 900 km and to extend north into Washington and south across most of Nevada (Figure 7). This matches the spatial and temporal pattern observed for dike formation and flood basalt eruption. Liu and Stegman (2012) suggest that melting beginning with subducted oceanic lithosphere and grading upward into oceanic crust can explain the petrology of the CRB. Hales *et al.* (2005) attributed the CRB to lithospheric delamination on the grounds that the region subsided prior to eruption.

Long *et al.* (2012) favor a model whereby trench rollback starting at ~ 20 Ma induced asthenosphere upwelling and back-arc extension provided eruptive pathways. Their view differs significantly from that of Liu and Stegman (2012) and Faccenna *et al.* (2010) who consider the lithosphere as passive. Long *et al.* (2012) consider that ongoing trench migration enables continued magmatism. They point out that the Juan de Fuca trench is currently retreating at ~ 35 mm/a, a period of rapid rollback that started at ~ 20 Ma. They conducted idealized laboratory experiments using glucose and a rigid fiberglass "plate" to study flow in the upper mantle and emphasized the spatio-temporal complexity in mantle flow, a view that contrasts with more common simplistic models. Pavlis *et al.* (2012), for example, suggest that the Farallon slab is in reality continuous, but the absence of high velocities interpreted as a slab tear are, instead, a region where the slab seismic signature has been neutralized by thermal effects. There is still no obvious explanation in the model of Long *et al.* (2012) for the narrowness of the Newberry trend, and an *ad hoc* upwelling has to be invoked to explain ESRP-Y volcanism.

5 HELIUM

There is a growing body of evidence that high-$^3He/^4He$ in surface lavas derives from mantle lithosphere, not from the deep mantle, and the case for the ESRP-Y zone is particularly strong. Historically, $^3He/^4He$ in ESRP-Y volcanics and thermal springs higher than MORB values has been widely cited to support a plume model (Craig et al., 1978; Kennedy et al., 1985; Welhan, 1981). The rationale attributes high-$^3He/^4He$ to a near-primordial region of the mantle. This region is postulated to have been uninvolved in mantle convection over the 4.5-billion-year lifetime of Earth and, thus, to have experienced little loss of primordial ^3He. As a result of the high concentration of ^3He, the value of $^3He/^4He$ was reduced only slowly by ^4He ingrowth compared with regions of the mantle that lost most of their ^3He through degassing. Because of the perceived need to place the postulated near-primordial region beyond involvement in shallow-mantle convection, its location is assumed, in that model, to be the core-mantle boundary. Such a model requires the postulated Yellowstone plume to be rooted in the deep mantle.

$^3He/^4He$ ratios higher than those of MORB nevertheless do not provide direct evidence for depth. Instead, they indicate a source that has experienced unusually slow reduction in the original value of ~ 200 R/Ra ($^3He/^4He$ normalized to the atmospheric value) of the young Earth. Simply put, they indicate an old source, not necessarily one that resided in the deep lower mantle.

There are difficulties with the deep model. A high concentration of ^3He in the deep mantle disagrees with high-temperature planetary accretion, which strongly degassed Earth in volatile elements and reduced the amount of He by many orders of magnitude. Also, if high-

$^3He/^4He$ were associated with an undegassed mantle region, then rocks with high-$^3He/^4He$ would be rich in He. In fact, the opposite is observed (Anderson et al., 2006; Moreira and Sarda, 2000; Ozima and Igarashi, 2000).

A slower-than-average reduction in $^3He/^4He$ over time could occur as a result of unusually slow ^4He ingrowth. This could occur, for example, via storage in a low-U+Th environment (Anderson, 1998a, b; Meibom et al., 2003; Meibom et al., 2005). Low-U+Th hosts include the residuum left after basalt melt is extracted from mantle peridotite (e.g., Brooker et al., 2003), recycled oceanic lithosphere, and olivine-rich cumulates (Natland, 2003). Individual olivine crystals, which are essentially devoid of U+Th, encapsulate gas bubbles that are largely CO_2 but also contain He. ^4He atoms generated by U+Th decay in surrounding minerals are not sufficiently energetic to penetrate the crystals and therefore do not lower $^3He/^4He$ in the bubbles. In addition, the diffusion of ^4He from surrounding materials into olivine crystals is hindered by differences in chemical potential. He is volatile but highly soluble in trapped CO_2-rich bubbles in olivine, and essentially insoluble in olivine itself. Thus, it will tend to be retained in bubbles in olivine crystals. This suggests a model whereby noble gases are trapped in olivine and pyroxene in cumulate olivine-gabbroic layers in the lowermost oceanic crust. Such a model could explain the high-$^3He/^4He$ in volcanics that contain a component of recycled oceanic crust.

Recently, new evidence has been presented for an origin for high-$^3He/^4He$ in the continental lithospheric mantle (Huang et al., 2014). $^3He/^4He$ values in the range ~ 5 - 22 R/Ra from a suite of postulated plume localities are anticorrelated with unradiogenic $^{206}Pb/^{204}Pb$, and correlated with unradiogenic $^{207}Pb/^{204}Pb$. The most internally consistent model to explain this is ancient sequestration of both He and Pb in unradiogenic sulfide melts that were co-precipitated with mafic cumulates (pyroxenites) during major melting episodes at the time of continental crust formation. The lack of U+Th in these cumulates, which do not partition into sulfides, would ensure preservation of ancient, high-$^3He/^4He$ isotope ratios. The cumulates are stored in the deep continental lithosphere, or have been delaminated over time and dispersed throughout the asthenosphere and upper mantle.

Recent work by Lowenstern *et al.* (2014) demonstrated that the copious ^4He degassed at Yellowstone must have its source in the Archaean lithosphere. It thus seems likely that ^3He too could have been stored in the lithospheric mantle to be liberated during the voluminous Quaternary volcanism. A model whereby the high-$^3He/^4He$ derives from basement geology and not a deep, primordial reservoir fits well the He-Pb systematics of the High Lava Plains and the ESRP-Y zone. This agrees with the strong seismic evidence that the source of ESRP-Y volcanics is the shallow mantle.

6 A PURE PLATE MODEL

There is a tendency to assume that the main factor needed to explain surface volcanism is melt in the mantle, and that involvement of the lithosphere is relatively unimportant. Lithosphere involvement is only invoked where spatial relations do not fit, and then phenomena such as 'upside down drainage', 'thin spots', 'ridge capture' or 'ridge escape' may be invoked (Keller et al., 2000; Mittelstaedt et al., 2011; Sleep, 1997). This amounts to suggesting that sub-lithospheric topography guides the lateral flow of rising melt–the lithosphere is still not viewed as controlling whether or not eruption occurs.

Here, we propose a pure plate model for CRB-ESRP-Y volcanism. Surface volcanism is attributed to extension of the lithosphere permitting the rise of pre-existing melt. Melt is viewed as being commonplace in the mantle, and its tendency to rise is not considered to be the primary cause of surface eruptions.

At 17 Ma, as the subduction zone to the west shortened with northward migration of the Mendocino triple junction leaving a slab window in the Farallon plate farther south, the CRB erupted in response to back-arc extension behind the downgoing plate from fissures parallel to the margin of the adjacent cratonic plate interior. The source of the melt may have been decompression upwelling of asthenosphere flooding through a slab tear, or large volumes of melt pre-existing at the lithosphere-asthenosphere boundary (Silver et al., 2006). Simultaneously, the basin-range region began to extend. Extension has not been distributed uniformly throughout the province, however, but is mostly taken up along two dominant, subparallel axes (e.g., Thatcher et al., 1999). We propose that the time-progressive chain of rhyolitic calderas in the ESRP-Y zone formed in response to the eastward migration of the easternmost of these axes of intense basin-range extension (Figure 8).

Throughout most of the basin-range province, extension is accompanied by relatively minor, commonly rhyolite-basalt volcanism (Christiansen and Lipman, 1972) . The ESRP-Y zone lies at a major lithospheric boundary where thin basin-range lithosphere is juxtaposed against thick lithosphere of the Northern Rocky Mountains and Idaho batholith. Across this zone, the rate of extension decreases abruptly over a distance of only 100 km. We propose that because of this the style of extension changes from ‘dry’ (normal-faulting) in the Great Basin region to ‘wet’ (magmatic) in the ESRP-Y zone (cf. Parsons et al., 1998).

Anders (1994) shows that migration of silicic volcanism on the ESRP-Y zone has gone hand-in-hand with accelerated normal-fault motion on large, range-bounding normal faults (Figure 9). Pierce and Morgan (2009) describe Cenozoic faulting south of the three youngest rhyolitic calderas of the ESRP-Y and also find that belts of fault activity have migrated NE in conjunction with the adjacent rhyolitic volcanism. These findings are reflected in current deformation studied using GPS surveying. At present, the most intense zones of extension accompany Holocene faults and lie near the western and eastern boundaries of the province. Little extension occurs across the central 500 km of the province (Thatcher et al., 1999). Our model proposes that rhyolitic volcanism along the ESRP-Y zone followed migration of the locus of most rapid extension, not vice versa. Importantly, the ESRP-Y zone existed in some form prior to the arrival of the axis of extreme extension. Its present-day manifestation formed along a pre-existing extensional zone—it did not form in initially inactive lithosphere.

GPS data have been collected locally in the ESRP-Y zone since 1990 (Chadwick et al., 2007; Puskas and Smith, 2009; Puskas et al., 2007; Rodgers et al., 2005). Assessing long-term averaged rates of motion is difficult because deformation is highly episodic. Major, time-varying deformations result from uplift and subsidence of the Yellowstone caldera and post-seismic viscoelastic deformation transients from large local earthquakes such as the 1959 M7.5 Hebgen Lake and the 1983 M7.3 Borah Peak earthquakes (Puskas et al., 2007). These motions cannot simply be subtracted from the long-term deformation field, however, because coseismic and post-seismic transient motions are intrinsic components of the time-averaged total motion (Foulger et al., 1992; Heki et al., 1993; Hofton and Foulger, 1996a, b).

Despite these problems, assessing regional variations in time-averaged motion has been attempted (Figure 10). The following is reported for the period 1987 - 2003 (Chadwick et al., 2007; Puskas and Smith, 2009; Puskas et al., 2007; Rodgers et al., 2005):

1. The Yellowstone plateau is extending at a rate of 2-5 mm/a;
2. The ESRP displays little measurable internal deformation; and
3. The rate of motion immediately north of the ESRP (~ 2.0 mm/a) is significantly lower than the rate just south of it (~ 3.4 mm/a).

Net extension in the Yellowstone area is consistent with the existence of a volcanic center there. Although little surface deformation is reported for the ESRP, extension must occur in the long term because it lies between zones to the south and north that are both extending via normal faulting. Extension via basaltic diking parallel to basin-range trends (Figure 11) has been discussed by Rodgers *et al.* (1990), Kunz *et al.* (1992), and Parsons *et al.* (1998). Northwesterly oriented Holocene volcanic rift zones traverse the ESRP and have erupted basalt flows–95% of the surface of the ESRP was covered by basalt in the past 730,000 a and about 13% within the last 15,000 a (Kunz et al., 1992). A time-averaged extension rate of a few mm/a would be sufficient, or about 10% of a slowly spreading plate boundary. Extension via diking is episodic, with brief periods of extension alternating with long periods of quiescence (e.g., Björnsson et al., 1977). It is thus unsurprising that deformation has not been captured in short-term GPS surveys. If the ESRP has deformed in this style throughout its lifetime, the width of the entire set of dikes emplaced must amount to ~ 35 km. The rates of motion measured using GPS are in broad agreement with geological observations which suggest that the long-term extension rates for the last few Ma are 2 mm/a north of the ESRP and 5 mm/a south of it (Anders, 1994; Christiansen et al., 2002; Rodgers et al., 2002).

Analogs for this situation occur elsewhere in the W USA. The Coso Hot Springs is a nascent core complex that forms at a right-stepping *en echelon* offset in the dextral strike-slip system of the Owens Valley (Monastero et al., 2005; Weaver and Hill, 1978). The resulting NW-directed transtension gives rise to normal and strike-slip faulting in the upper few kilometers of crust and ductile stretching, permitting shallow igneous intrusions to rise, beneath (Monastero et al., 2005).

A larger example is Long Valley caldera at the northern end of Owens Valley. This volcanic field is orders of magnitude more voluminous than other volcanic localities nearby. It has been active for the last ~ 3 Ma, culminating in a giant 600-km^3 caldera-forming rhyolitic eruption at 760,000 a. This is ~ 25% of the volume of the massive 2,500 km^3 Huckleberry Ridge Tuff that erupted from Yellowstone at 2.2 Ma. Like the ESRP-Y zone, Long Valley has erupted compositions ranging from rhyolite to basalt. Hill (2006) and Riley *et al.* (2012) present a model whereby Long Valley caldera formed in an area of lithospheric dilation induced by regional fault movements. Specifically, block kinematics predict dilatation between the Sierra Nevada, Adobe and Owen Valley blocks, inducing mantle to upwell (Riley et al., 2012).

The combination of rhyolitic caldera volcanoes and fissures erupting basaltic lava on the ESRP is reminiscent of the so-called ‘volcanic systems’ of Iceland. Icelandic volcanic systems comprise fissure swarms, each containing a central volcano erupting both rhyolite and basalt. The spreading plate boundary crossing Iceland comprises *en echelon* arrays of such spreading centers. Along the ESRP-Y zone, voluminous rhyolitic caldera volcanoes and fissures erupting basalt lie side-by-side, forming a chain oriented parallel to the direction of lithospheric extension. This contrasts with the situation in Iceland, where the volcanic systems form *en echelon* chains oriented roughly perpendicular to the direction of extension (Figure 12). The explanation for this may be that, whereas oceanic spreading plate boundaries form by propagation of rifts perpendicular to the direction of spreading, the ESRP has formed by propagation of basin-range extension parallel to the direction of extension. Thus, a volcanic zone has formed that comprises an array of systems analogous to Icelandic volcanic system that lie side-by-side and not end-to-end.

An example of a laterally migrating Icelandic volcanic system is the Hengill-Grensdalur complex in the southwest. This area is a ridge-ridge-transform triple junction and lies at a locality where thin crust underlying the ridge branches meets thicker crust underlying the transform branch. Lateral migration of the locus of volcanism occurred at ~ 0.5 Ma, when the then-active Grensdalur volcanic system became extinct and the currently active Hengill volcanic system developed ~ 5 km further to the west (Figure 12) (Foulger, 1988a, b; Foulger and Toomey, 1989; Miller et al., 1998).

7 SYNTHESIS AND DISCUSSION

7.1 Plume models for Yellowstone

Notwithstanding the most fortuitous location and the most sophisticated seismological experiment ever staged, seismic evidence in support of a Yellowstone plume is underwhelming. None of the many tomography models produced to date show repeatable evidence for a vertically extensive low-velocity body extending down into the lower mantle, accompanied by deflections on the TZ discontinuities (Fouch, 2014). This adds to the many geological details of CRB-ESRP-Y volcanism that do not fit a plume model without special pleading (Section 2).

A mantle-plume origin for CRB-ESRP-Y volcanism is nevertheless still assumed by some workers. It is important to appreciate that the plume model cannot be disproven because it is so conveniently flexible. Any mismatch between prediction and observation of spatial or temporal variations in volcanism can be explained simply by distorting and pulsing in the mantle. Thus, for example, Camp and Ross (2004) suggest the Newberry zone results from a backward-flowing arm of a plume beneath Yellowstone. The excessive rate of migration required by the postulated plume tail for the period 10 - 17 Ma has been attributed to westward deflection of a plume head by the Farallon slab (Pierce and Morgan, 2009), or the 'snapping' to an upright position of a plume after escape from the Juan de Fuca plate (Geist and Richards, 1993). Such *ad hoc* models may be far removed from realistic mantle dynamics, and furthermore, any such model embellishments must be testable. The lithosphere-delamination model suggested by Hales *et al.* (2005) to explain observed precursory subsidence was countered by Pierce and Morgan (2009) who suggest that the delamination was triggered by an arriving plume head.

The original plume model of Morgan (1971; 1972a; 1972b) provided an elegant, testable hypothesis for apparently fixed, time-progressive volcanic chains, and it inspired much productive research on some of the most interesting geological provinces on Earth. This research quickly produced new observations that prompted the addition of empirically based correlatives of the original concept. These included laterally extensive flood basalts, rapid emplacement rates, ocean-island-type geochemistry (Hanan and Schilling, 1997; Hart et al., 1992; Hofmann, 1997; Schilling, 1973), and high $^3He/^4He$ ratios (Craig and Lupton, 1981). There has, however, been insufficient skepticism of these empirical correlations, and they have tended to give rise to circular reasoning. Thus, when such observations were made where a plume was interpreted, they were assumed to characterize plumes, and when discovered elsewhere, they were taken to demonstrate that a plume must be present there as well. For example, high $^3He/^4He$ ratios were originally observed at Hawaii and were proposed to be a plume characteristic (Craig and Lupton, 1981). When observed at Yellowstone, such ratios were then cited as conclusive evidence for a plume irrespective of evidence to the contrary.

In the case of the CRB, the huge area covered is frequently cited in support a plume-head model (e.g., Faccenna et al., 2010). Indeed, 'large igneous provinces' (LIPs), often assumed to represent plume-head volcanism, are defined by surface area, not by the total volume of magma emplaced (Coffin and Eldholm, 1994). Nevertheless, the area covered is a function of the topography at the time of eruption, not just of the volume erupted. The main eruptive phase of the CRB lasted ~ 1.6 Ma and produced 234,000 km^3 of lava. Such rapid emplacements are frequently cited as evidence of plumes despite numerical modeling that shows that the generation of such a volume of melt in a rising, decompressing plume head would take 10-20 Ma (Farnetani and Richards, 1994).

Ocean-island-type geochemistry is explained by the incorporation of fusible, subducted, near-surface materials in the source (Hofmann and White, 1982). High-pressure melting experiments on the most primitive rock compositions of the Grande Ronde basalt suite show that the entire compositional range of the melts can be explained by melting of up to 30-50% of a MORB-like source at ~ 20 GPa (~ 70 km depth) at a normal mantle temperature of 1300 - 1350˚C (Takahahshi et al., 1998).

7.2 Tomography and geochemistry

Despite many major seismic studies of the ESRP-Y region, researchers are still divided regarding whether or not a mantle plume underlies Yellowstone. Seismology has not resolved this perennial question. This suggests that seismic tomography, as conventionally practiced, cannot test the plume hypothesis. In the case of Yellowstone, the experimental conditions are the best likely to be achievable anywhere on Earth in the foreseeable future. The region is optimally located in the interior of a continent, surrounded on all sides by the most ambitious seismic network ever deployed as well as several targeted, local dense arrays. This contrasts with most melting anomalies which are located on oceanic islands. Despite its optimal setting, seismic tomography images of Yellowstone are insufficiently repeatable to unite the scientific community on the question of the existence of a plume. Regardless of one's preferred model, evidence to support it can be found somewhere within the wide suite of inversion results available.

Although seismology can yield much remarkable information about the interior of Earth, it alone probably is fundamentally unable to resolve the question of whether deep mantle plumes exist. The absence of low velocities is typically not a possible finding since seismic tomography results are generally presented as deviations from the regional mean. Images of the results are thus constrained to show both high and low velocities in equal amounts (Foulger et al., 2013). Furthermore, there is always a lower limit in size and strength of anomalies that can be resolved, and it will always be possible to propose plumes that are too weak or narrow to be detected.

The message from geochemistry is similar (Lustrino and Anderson, 2015). Geochemistry has essentially no power to resolve depth. Proposed geochemical associations with the deep mantle are based entirely on theories concerning the postulated locations of the sources of particular geochemical signatures. In the case of $^3He/^4He$, the assertion that high values indicate a plume is rooted in an initial empirical correlation with Hawaii which was followed by a theory erected to explain how it could arise from the core-mantle boundary (Craig and Lupton, 1981).

7.3 Final remarks

Many plume models for Yellowstone are logically flawed. All models for mantle dynamics in the W USA call for substantial complexity in the mantle flow field. This is at odds with a plume explanation for the time-progressive chain of rhyolitic volcanoes. Ironically, what is considered the strongest evidence for a plume thus counts against the model (Fouch, 2014). Time progression, showing relative fixity to the Hawaiian volcanic locus, and high-$^{3}He/^{4}He$, are only explained in the plume model by a source at the core-mantle boundary. There is no reason why ‘upper-mantle plumes’ (e.g., Xue and Allen, 2010), ‘TZ plumes’ (e.g., Fee and Dueker, 2004) and the numerous variants proposed to be related to subducting-slab processes (e.g., Faccenna et al., 2010) should produce time-progressive volcanism fixed relative to Hawaii. A more reasonable explanation for the approximate relative fixity of the Hawaiian and Yellowstone melt loci for the last few Ma is that both are fixed relative to the global plate boundary system, as predicted by the plate hypothesis.

Referring to purported upper-mantle diapirs as ‘plumes’ introduces confusion. Semantics are influential (Faccenna et al., 2010; Long et al., 2012). Constructive discussions require well-defined and uniformly understood terminology. The time-progressive Newberry trend is generally attributed to plate-boundary-related processes. If plate-related processes can cause time progression in this volcanic chain, there is no reason why they cannot do the same for the ESRP-Y zone. The fact that its azimuth is parallel to the direction of plate motion is not proof of a deep-mantle plume.

Voluminous rhyolitic volcanism along the ESRP-Y zone followed migration of the locus of most rapid extension, not vice versa (Anders, 1994). Models that consider the volcanism to have initiated the large range-bounding faults in the neighborhood seek to separate out the effects of the purported plume from basin-range deformation. This would imply that these faults are independent of, and unrelated to, basin-range extension further south, which is implausible. The entire tectonomagmatic system that includes the CRB, the High Lava Plains, the ESRP-Y zone and the widespread volcanism throughout the W USA calls for a holistic explanation involving the subducting Farallon slab, the complexities of plate-boundary evolution, and the development of the vast back-arc extensional region (Fouch, 2014). Models that involve separate and unrelated elements—*dei ex machina*—are unconvincing. The extreme seismic anomalies beneath the ESRP-Y zone may have developed from the top down, growing downward and outward, in response to extraction of melt and volatiles at the surface inducing replacement by compensating upwelling of melt and volatiles from below. Small-scale analogies are the depletion zones in exploited geothermal or hydrocarbon reservoirs, which grow downward and outward from the fluid extraction loci (Gunasekera et al., 2003). Future advances are unlikely to come from the results of any one single technique, but in the application of sound scientific logic to the multidisciplinary observations, and testing of clearly defined, competing hypotheses.

Acknowledgments

The authors gratefully acknowledge valuable and stimulating discussions with Bruce Julian, Alex Peace, Ken McCaffrey and Jonny Imber. Jeroen Ritsema and Robert van der Hilst kindly shared their seismic models and plotting software. The manuscript was improved in the light of two anonymous reviews.

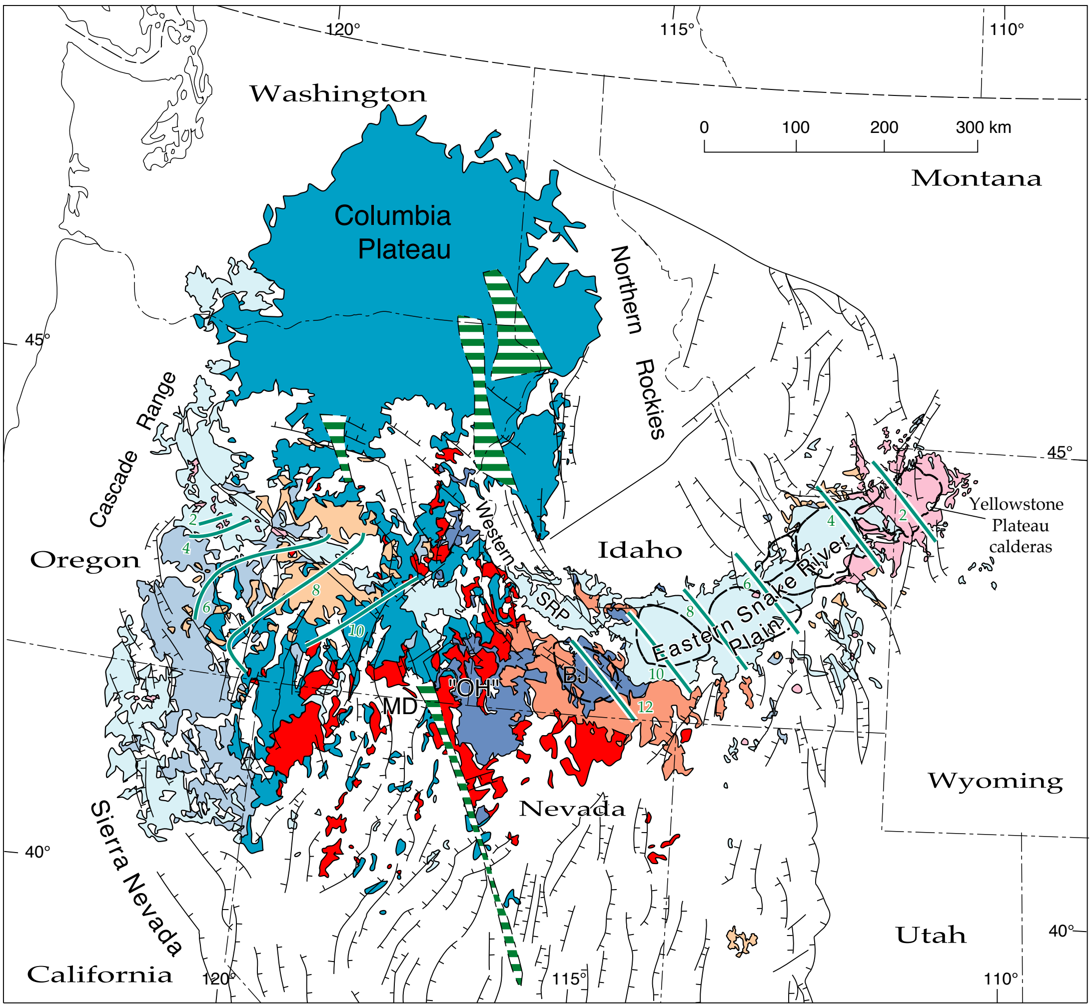
Washington
Columbia Plateau
Northern Rockies
Montana
0 100 200 300 km
Cascade Range
Oregon
Western SRP
Idaho
Eastern Snake River Plain
Yellowstone Plateau calderas
MD
"OH"
BJ
Nevada
Wyoming
Sierra Nevada
California
Utah
120°
115°
110°
45°
40°

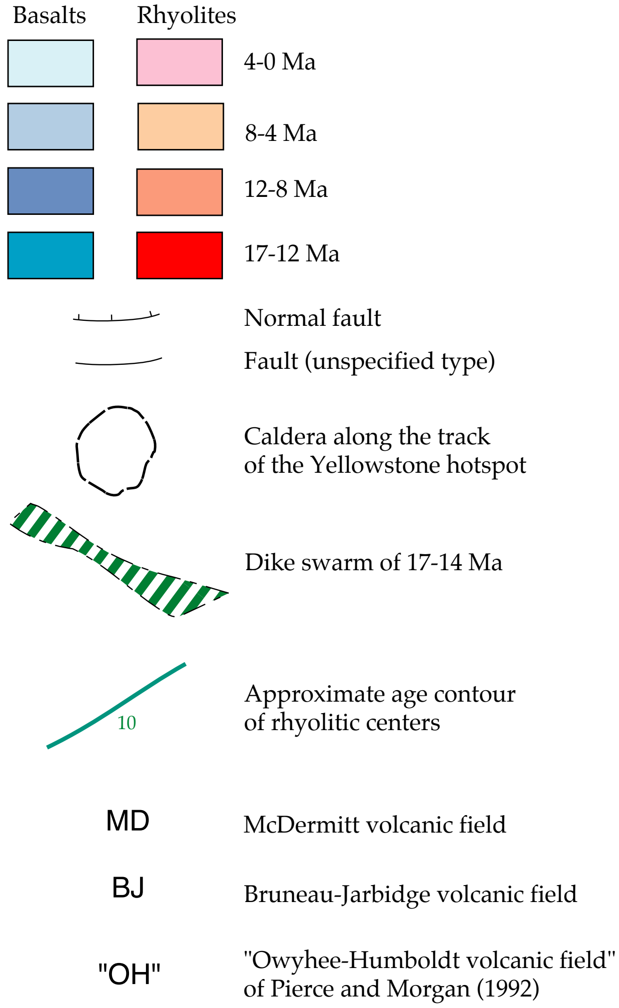

Figure 1: Map of the northwestern United States showing basin-range faults, and basalts and rhyolites of 17 Ma and younger. Approximate age contours of rhyolitic volcanic centers (~12, 10, 8, 6, 4, and 2 Ma) across the northeast-trending Eastern Snake River Plain are shown. A contemporaneous trend of oppositely propagating rhyolitic volcanism that trends northwest across central Oregon is indicated by similar contours. Locations of calderas are from Pierce and Morgan (1992) and Christiansen (2001) (from Christiansen et al., 2002).

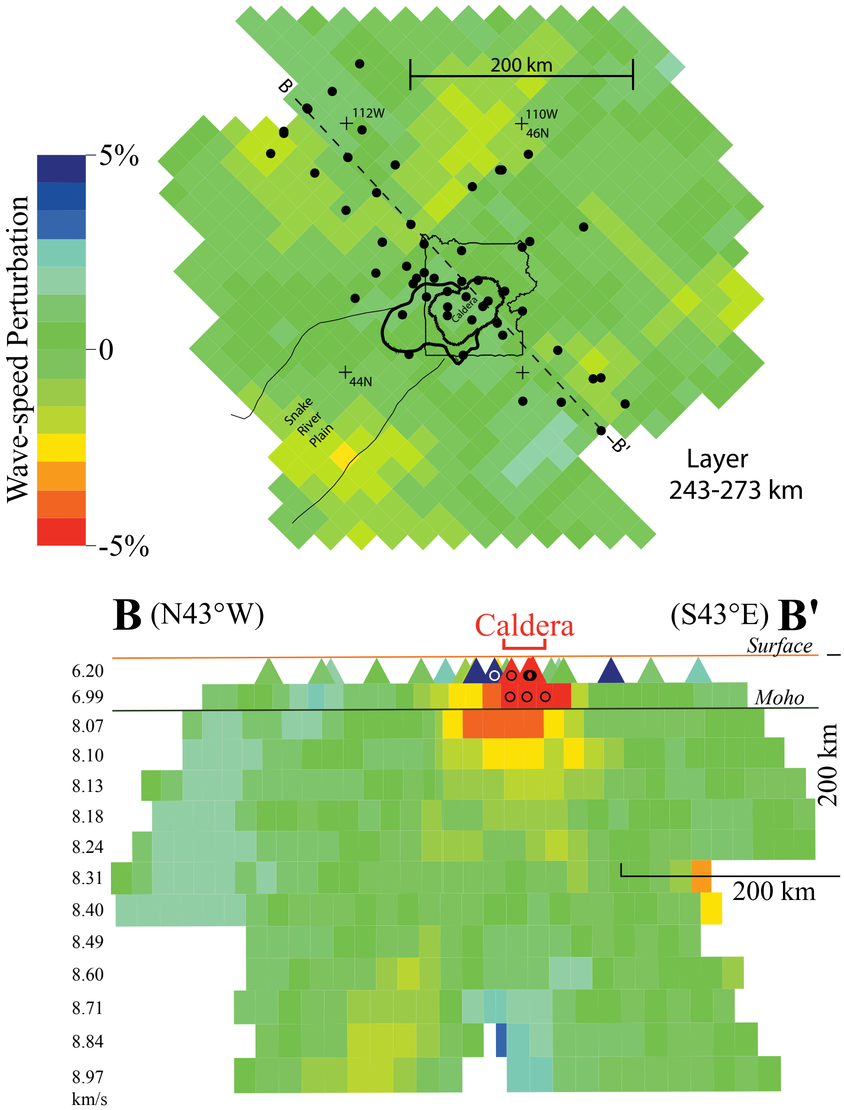

Figure 2: Teleseismic tomographic V_P structure beneath Yellowstone. Top: dots show the seismic stations used, the boundary of Yellowstone National Park, the calderas of the Yellowstone Plateau volcanic field, the edges of the eastern Snake River Plain, and line of cross section BB' shown in lower panel. Colors in top panel indicate wave-speed variations in the depth interval 243–273 km, where a deep plume-like structure would be imaged if one exists. Lower panel: cross section through the model at the northeast edge of the caldera (from Christiansen et al., 2002).

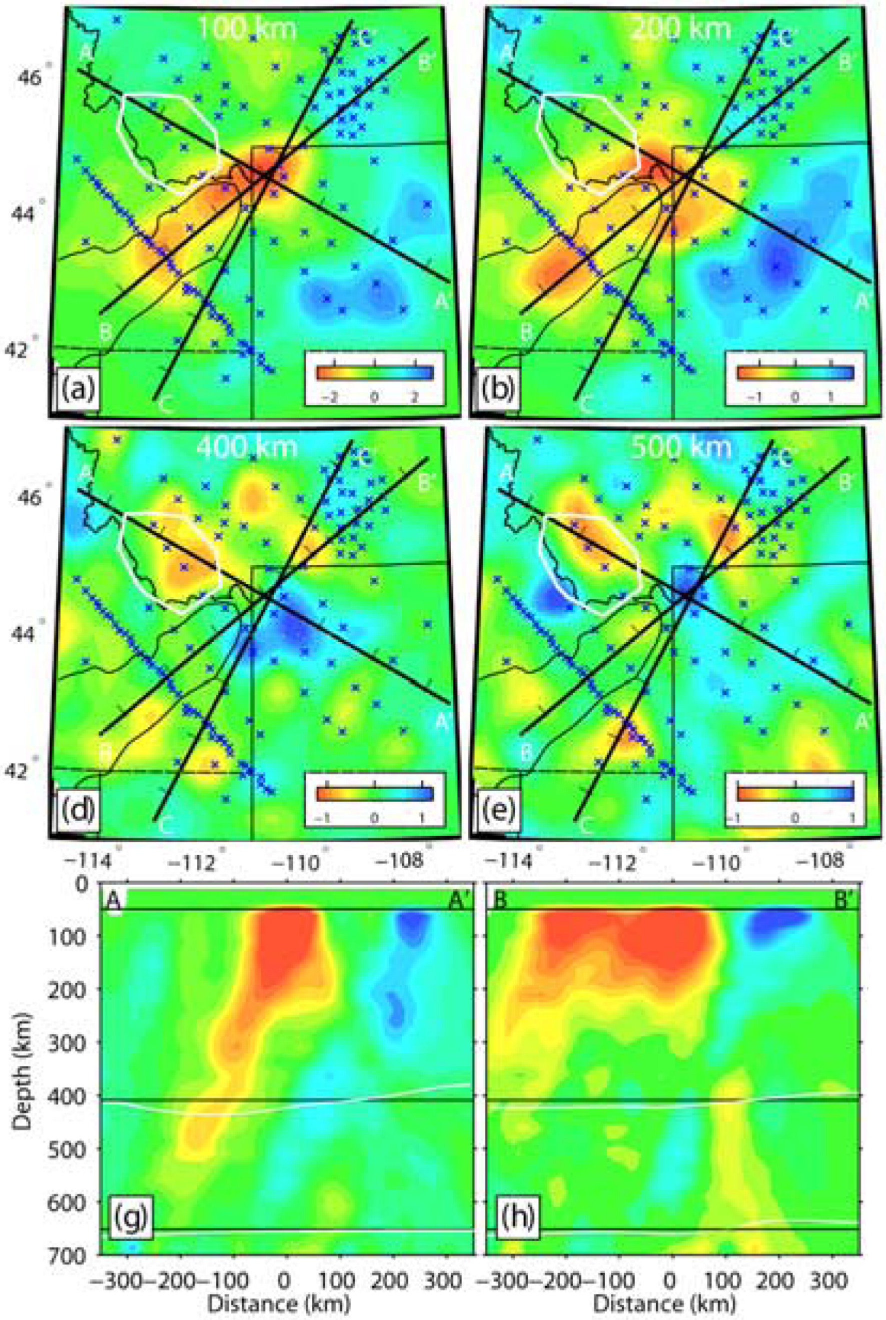

Figure 3: Teleseismic tomography V_P structure beneath Yellowstone (from Yuan and Dueker, 2005). White rings on the horizontal sections indicate where the 410-km discontinuity is depressed. In the cross sections in the lower panels, the 410- and 650-km discontinuities are shown by white lines, and their average depths by black lines (Fee and Dueker, 2004).

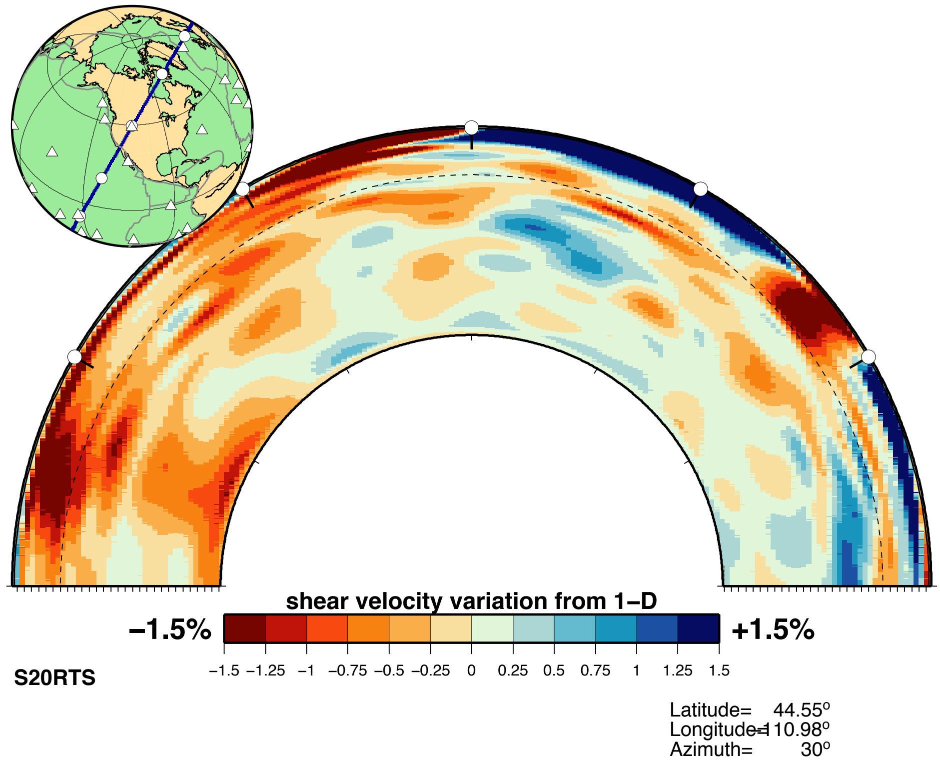

Figure 4: NE-SW cross section through the Yellowstone caldera, showing the mantle tomography model of Ritsema *et al.* (1999).

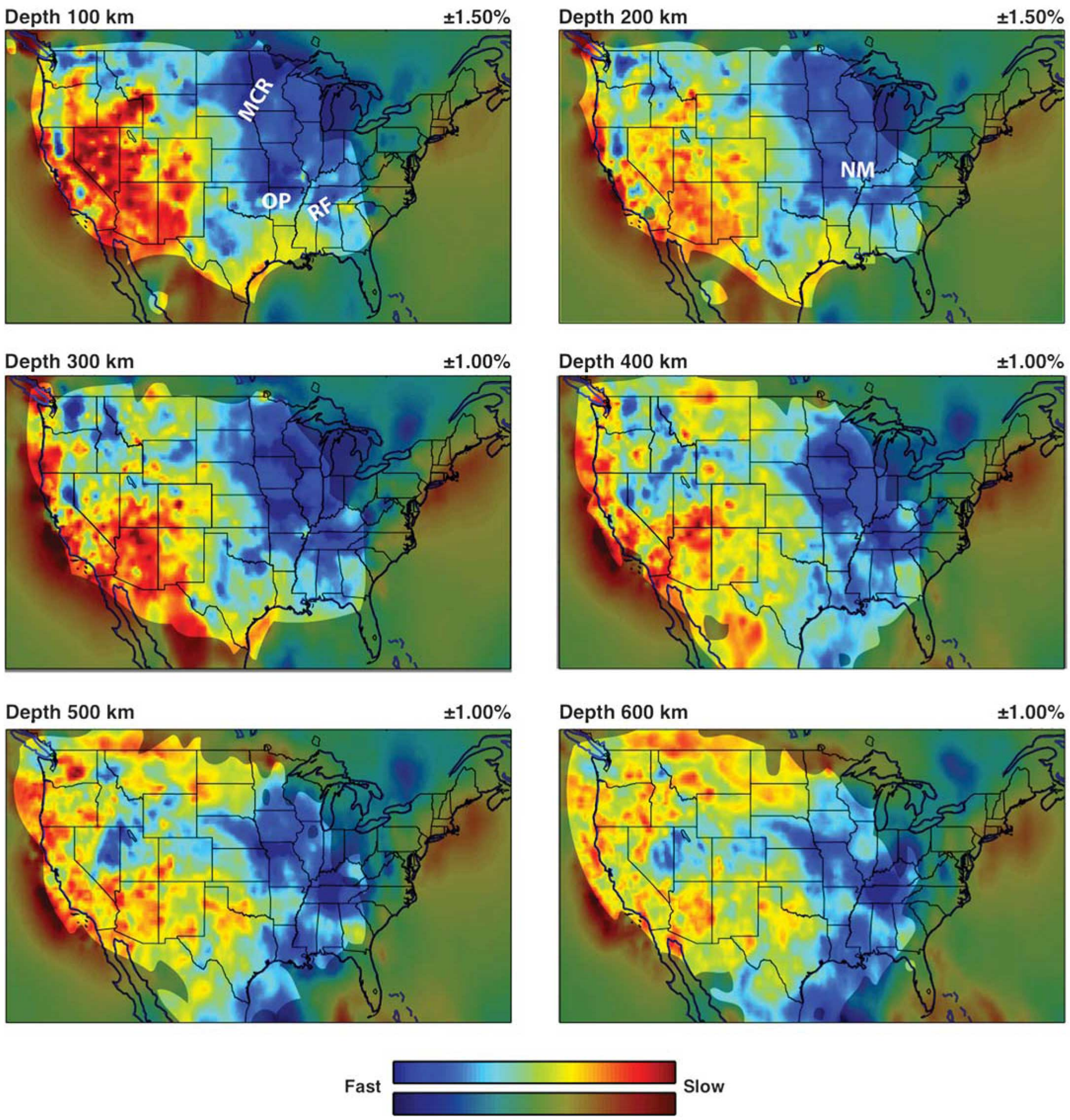

Figure 5: Lateral variations in V_P according to model MITP_USA_2013JAN at 100, 200, 300, 400, 500, and 600 km depth in the mantle beneath North America. Note that the 100- and 200-km depth slices are saturated at ±1.5% velocity anomaly, and the other depths at ±1%. MCR: Midcontinent Rift; OP: Ozark Plateau; RF: Reelfoot Rift; NM: New Madrid Seismic Zone. In the slice at 100 km depth, the three tongues of low velocity that trend NE under the W USA and underlie, from north to south, the ESRP-Y, St. George, and Valles volcanic zones, are particularly clear (from Burdick et al., 2014).

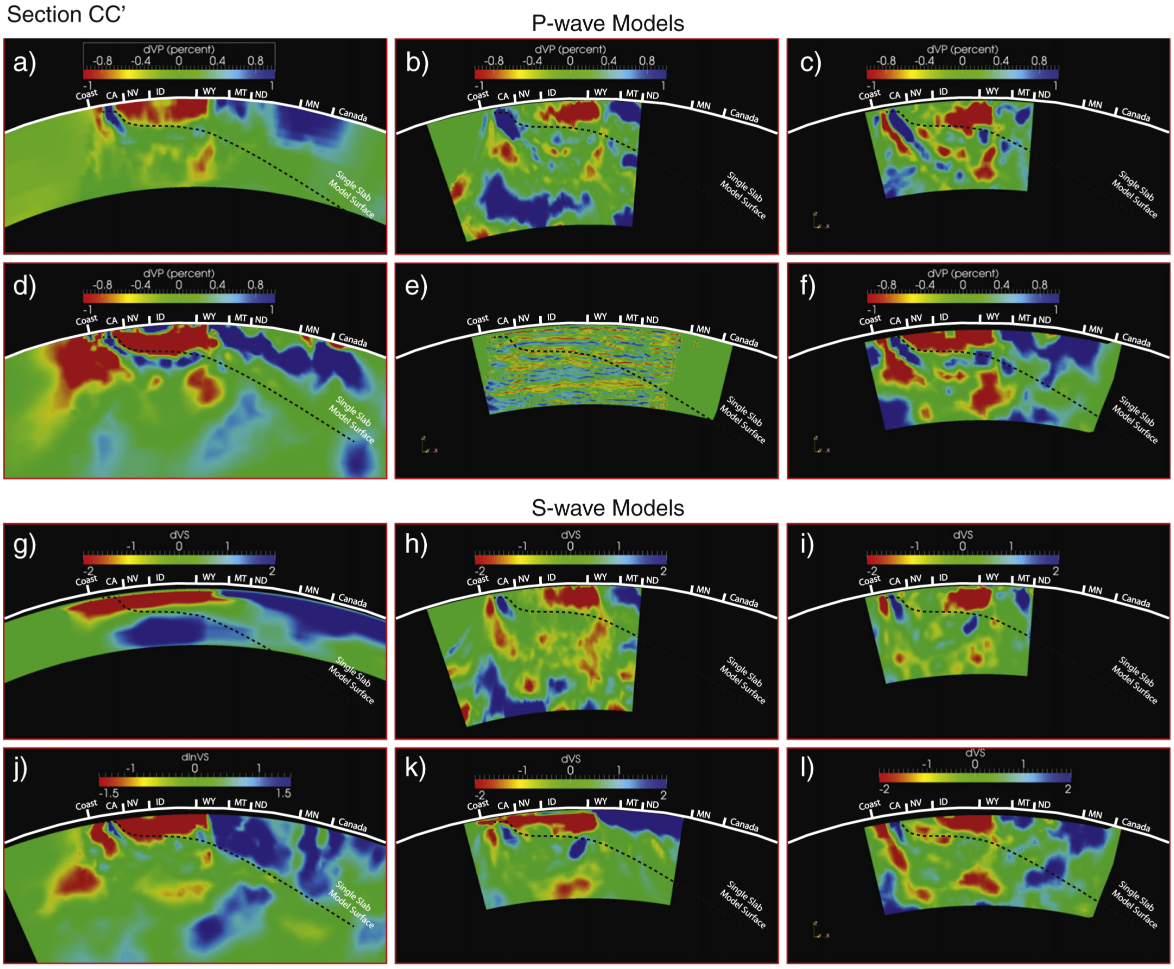

Figure 6: Cross section through the western USA running from Cape Mendocino to the Canada–Minnesota border. Sections are viewed from the southeast and slice the same section of each volume. The white line on each section is Earth's surface with geographic boundaries marked by radial, white colored ticks. States are defined by standard two character postal abbreviations. Tomography models all show high velocities as blue and low velocities as red with the scale shown on each section. The scattered wave image result (e) shows positive P-to-S conversion scattering potential in red and negative conversion as blue. V_P tomography results are as follows: (a) MIT11, (b) NWUS11-P, (c) DNA09P, (d) SIG11, (f) UOP (e) PWMIG11. V_S tomography results in the lower panel are (g) NA07, (h) NWUS11-S, (i) DNA09S, (j) TIA10, (k) DNA10, (l) UO10S. See Pavlis *et al.* (2012) for further details.

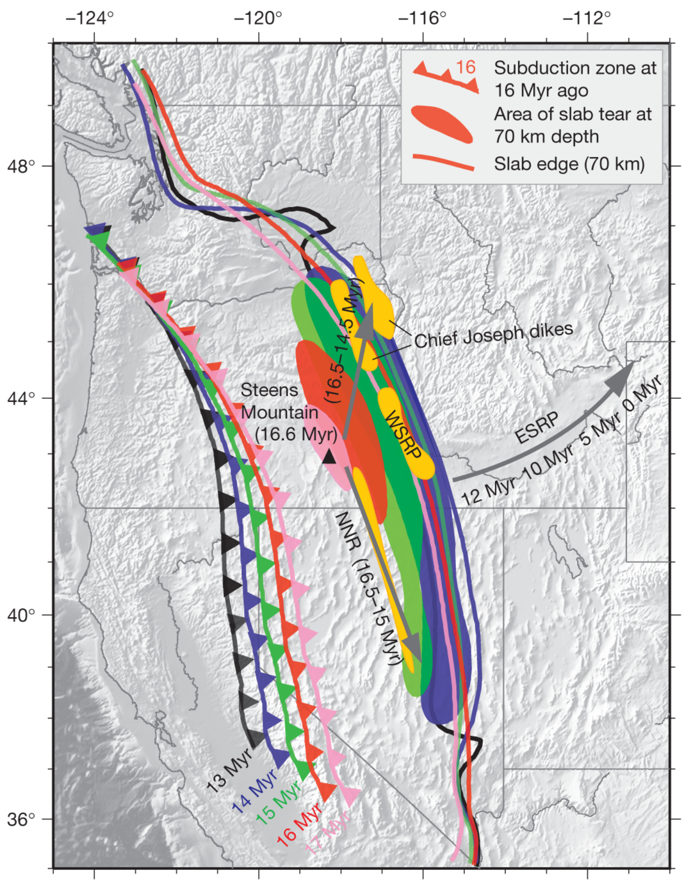

Figure 7: Development of the Farallon slab rupture beneath the western USA showing geometry of Farallon subduction at different times. Both the slab edge (solid lines) and slab gap (filled area) are shown at a depth of 70 km. Major volcanic dike swarms are shown in yellow. WSRP, western Snake River plain; ESRP, eastern Snake River plain; NNR, northern Nevada rift zone (from Liu and Stegman, 2012).

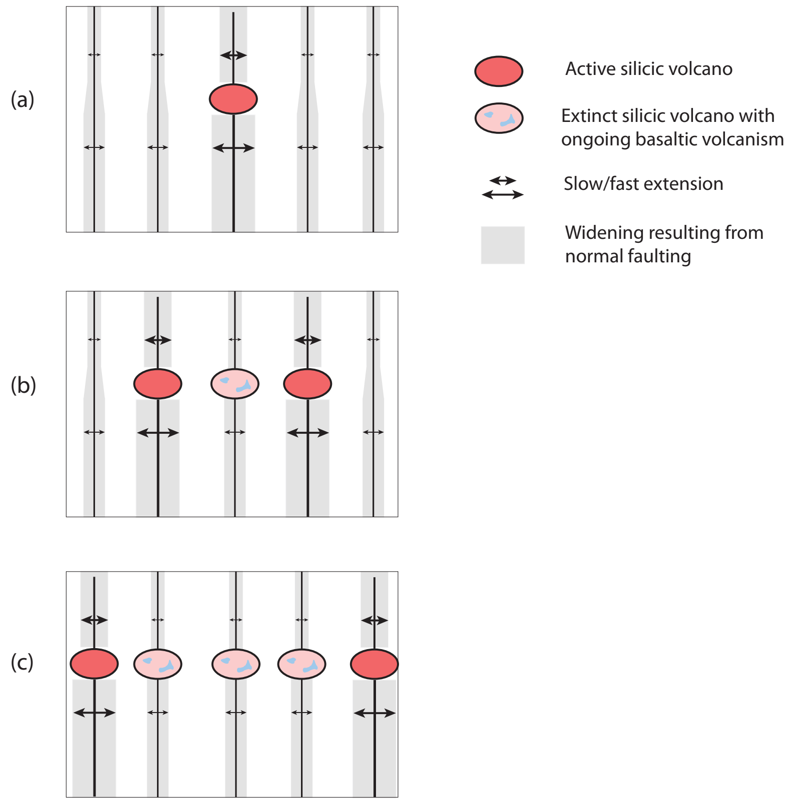

Figure 8: Schematic figure illustrating a model whereby the time-progressive chain of rhyolitic calderas in the ESRP-Y zone (rhyolitic volcanism ongoing - red, rhyolitic volcanism extinct - pink) formed in response to the eastward migration of the axis of most intense basin-range extension. The complimentary 'Newberry trend' formed by westward migration. Time increases (a) - (c).

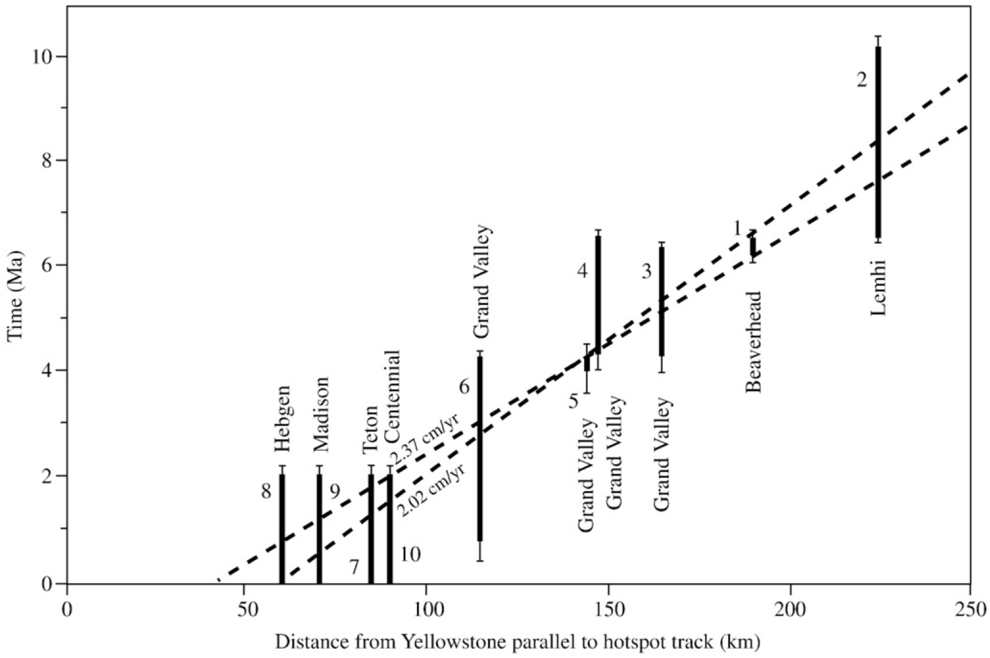

Figure 9: Migration of high fault displacements on large range-bounding normal faults in the vicinity of the ESRP-Y (after Anders, 1994). The rate of migration of high fault activity is 2.02 - 2.37 km/Ma, similar to the migration rate of large caldera-forming volcanism from 10 to 2 Ma.

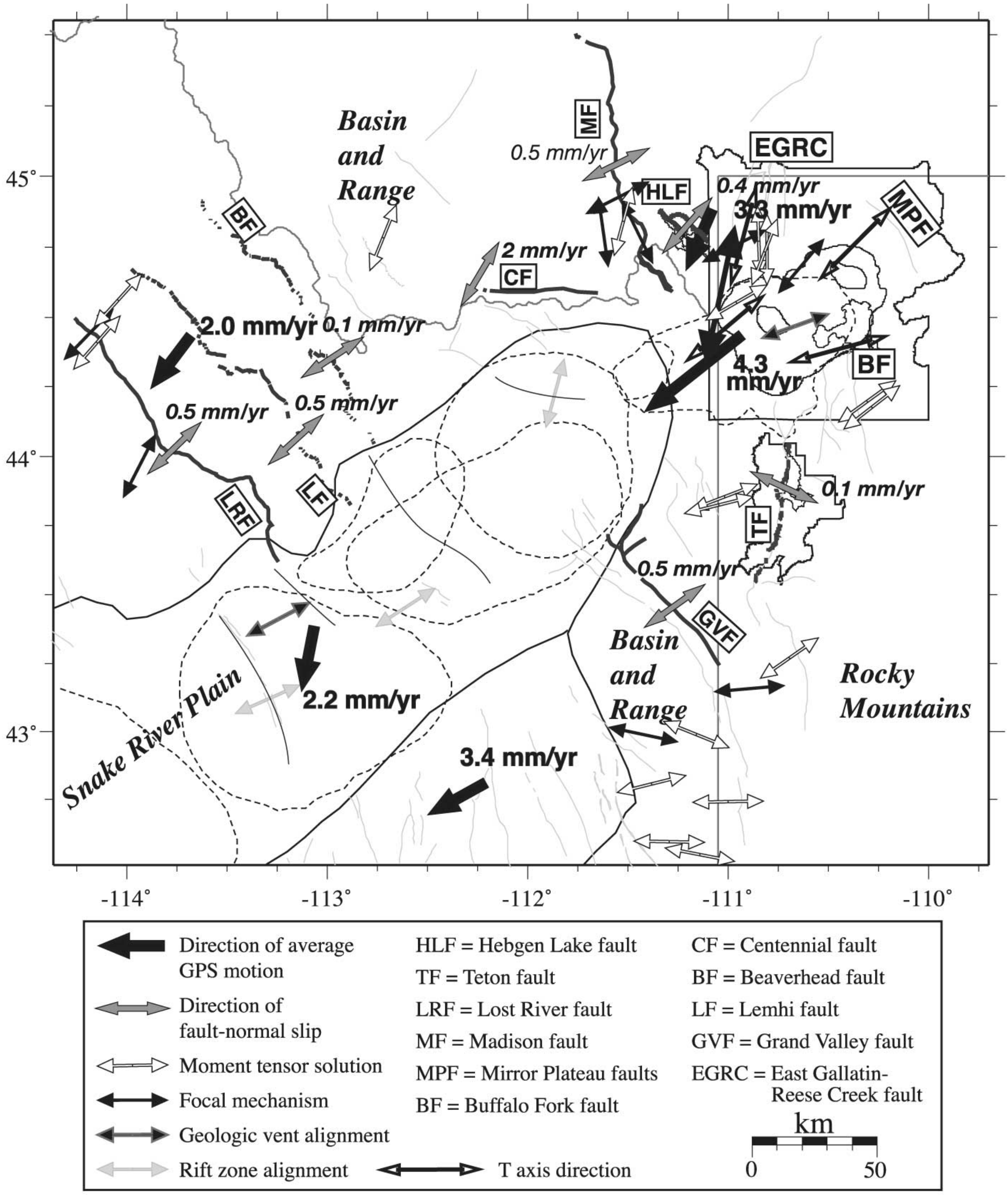

Figure 10: Summary map of GPS-measured deformation vectors for the Eastern Snake River Plain and Yellowstone. Average GPS rates are labeled in large font. For comparison, minimum principal stress indicators from other studies are also shown (from Puskas et al., 2007).

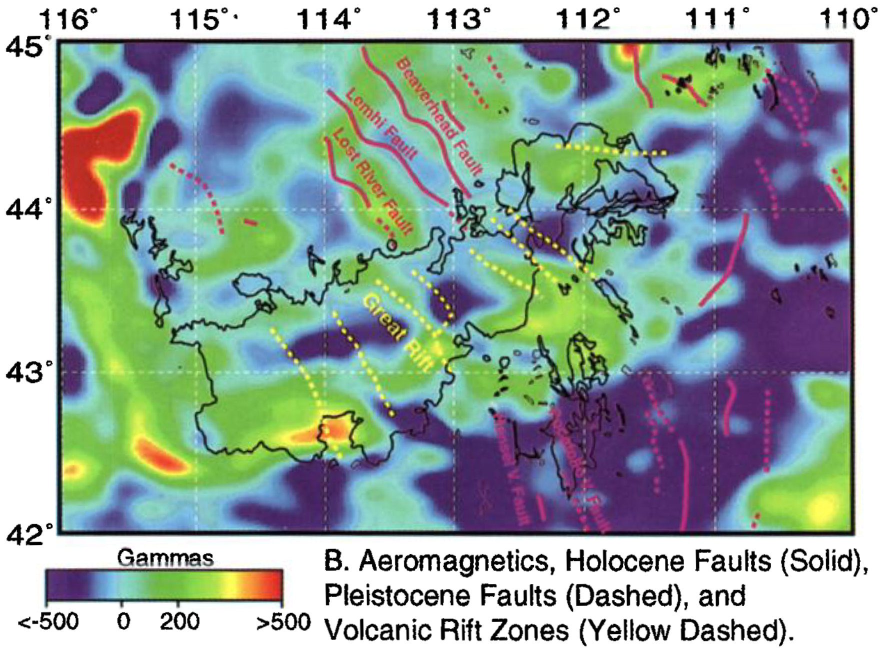

Figure 11: Aeromagnetic map of the Eastern Snake River Plain and Yellowstone region. Black line outlines the area of young basalt flows. Yellow dashed lines indicate volcanic rift zones. Major faults with Quaternary (solid red) and Pleistocene (dashed red) offsets are shown (from Parsons et al., 1998).

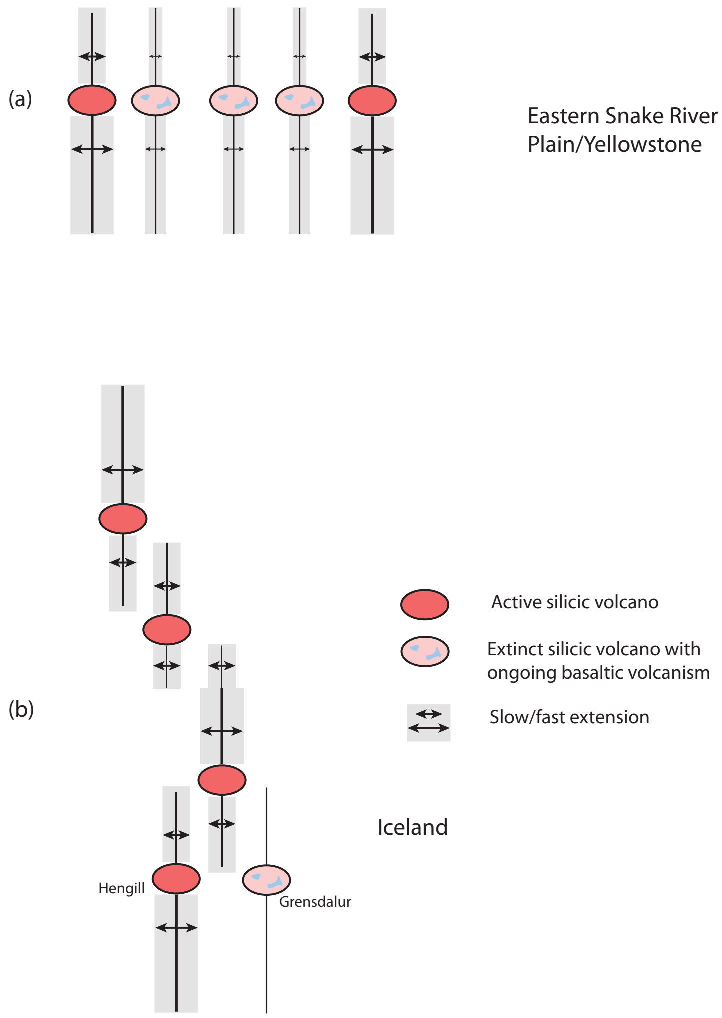

Figure 12: Schematic figure comparing the Eastern Snake River Plain and Yellowstone to the spreading plate boundary in Iceland, where the basaltic/rhyolitic volcanic systems typically form *en echelon* arrays oriented perpendicular to the direction of extension. (a) is panel (c) from Figure 8, (b) represents an array of volcanic systems forming a volcanic zone in Iceland.

References

Adams, D. C., and Humphreys, E. D., 2010, New constraints on the properties of the Yellowstone mantle plume from P and S wave attenuation tomography: Journal of Geophysical Research, v. 115, no. B12311.

Ander, M. E., Goss, R., and Strangway, D. W., 1984, A detailed magnetotelluric/audomagnetotelluric study of the Jemez volcanic zone, New Mexico: Journal of Geophysical Research, v. 89, no. B5, p. 3335-3353.

Anders, M. H., 1994, Constraints on North American plate velocity using the Yellowstone hotspot deformation field: Nature, v. 369, p. 53-55.

Anderson, D. L., 1998a, The helium paradoxes: Proceedings of the National Academy of Sciences of the United States of America, v. 95, p. 4822-4827.

-, 1998b, A model to explain the various paradoxes associated with mantle noble gas geochemistry: PNAS, v. 95, no. 16, p. 9087-9092.

Anderson, D. L., 2011, Hawaii, boundary layers and ambient mantle–geophysical constraints: Journal of Petrology.

Anderson, D. L., and Dziewonski, A. M., 1984, Seismic tomography: Scientific American, v. 251, p. 60-68.

Anderson, D. L., Foulger, G. R., and Meibom, A., 2006, Helium: Fundamental models, Volume http://www.mantleplumes.org/HeliumFundamentals.html: http://www.mantleplumes.org/, G. R. Foulger.

Becker, T. W., 2012, On recent seismic tomography for the western United States: Geochemistry Geophysics Geosystems, v. 13, no. Q01W10.

Beucler, E., Chevrot, S., and Montagner, J. P., 1999, The Snake River Plain experiment revisited: Relationships between a Farallon plate fragment and the transition zone: Geophysical Research Letters, v. 26, p. 2673–2676.

Bina, C., and Helffrich, G., 1994, Phase transition Clapeyron slopes and transition zone seismic discontinuity topography: Journal of Geophysical Research, v. 99, p. 15853-15860.

Björnsson, A., Saemundsson, K., Einarsson, P., Tryggvason, E., and Grönvold, K., 1977, Current rifting episode in north Iceland: Nature, v. 266, p. 318-323.

Boerner, D. E., Craven, J. A., Kurtz, R. D., Ross, G. M., and Jones, F. W., 1998, The Great Falls tectonic zone: Suture or intracontinental shear zone?: Canadian Journal of Earth Sciences, v. 35, p. 175-183.

Brooker, R. A., Heber, V., Kelley, S. P., and Wood, B. J., 2003, Noble gas partitioning behaviour during mantle melting: A possible explanation for “The He Paradox”?: EOS, Transactions of the American Geophysical Union, v. AGU Fall Meet. Suppl., p. V31F-03.

Bull, W. B., 1991, Geomorphic response to climatic change, New York, Oxford University Press, 326 p.:

Burdick, S., van der Hilst, R. D., Vernon, F. L., Martynov, V., Cox, T., Eakins, J., Karasu, G. H., Tylell, J., Astiz, L., and Pavlis, G. L., 2012, Model update March 2011: Upper mantle heterogeneity beneath North America from travel time tomography with global and USArray transportable array data: Seismological Research Letters, v. 83, p. 23-28.

-, 2014, Model update January 2013: Upper mantle heterogeneity beneath North America from travel time tomography with global and USArray transportable array data: Seismological Research Letters, v. 85, p. 77-81.

Camp, V. E., 2013, Origin of Columbia River Basalt: Passive rise of shallow mantle, or active upwelling of a deep-mantle plume, *in* Reidel, S. P., Camp, V. E., Ross, M. E., Wolff, J. A., Martin, B. S., Tolan, T. L., and Wells, R. E., eds., The Columbia River Basalt Province, Volume 497, p. 181-199.
Camp, V. E., and Ross, M. E., 2004, Mantle dynamics and genesis of mafic magmatism in the intermontane Pacific Northwest: Journal of Geophysical Research, v. 109, no. B08204.
Campbell, I. H., 2007, Testing the plume theory: Chemical Geology, v. 241, p. 153-176.
Chadwick, D. J., Payne, S. J., Van Hove, T., and Rodgers, D. W., 2007, Contemporary tectonic motion of the eastern Snake River Plain: A campaign global positioning system study: Tectonics, v. 26, no. TC6005.
Christiansen, R. L., 2001, The Quaternary and Pliocene Yellowstone Plateau volcanic field of Wyoming, Idaho, and Montana, Washington, United States Government Printing Office, U.S. Geological Survey Professional Paper, 144 p.:
Christiansen, R. L., Foulger, G. R., and Evans, J. R., 2002, Upper mantle origin of the Yellowstone hotspot: Bull. Geol. Soc. Am., v. 114, p. 1245-1256.
Christiansen, R. L., and Lipman, P. W., 1972, Cenozoic volcanism and plate-tectonic evolution of the Western United States: Part 2, Late Cenozoic: Royal Society of London Philosophical Transactions, ser. A, v. 271, p. 249-284.
Christiansen, R. L., and McKee, E. H., 1978, Late Cenozoic volcanic and tectonic evolution of the Great Basin and Columbia Intermontane region, *in* Smith, R. B., and Eaton, G. P., eds., Cenozoic tectonics and regional geophysics of the western Cordillera, Volume Memoir 152, Geological Society of America, p. 283-312.
Christiansen, R. L., and Yeats, R. S., 1992, Post-Laramide geology of the U.S. Cordilleran region, *in* Burchfiel, B. C., Lipman, P. W., and L, Z. M., eds., The Cordilleran orogen: Conterminous U. S.: Boulder, Colorado, Geological Society of America, p. 261-406.
Coffin, M. F., and Eldholm, O., 1994, Large igneous provinces: crustal structure, dimensions and external consequences: Reviews of Geophysics, v. 32, p. 1-36.
Cordery, M. J., Davies, G. F., and Campbell, I. H., 1997, Genesis of flood basalts from eclogite-bearing mantle plumes: Journal of Geophysical Research, v. 102, p. 20,179-120,197.
Courtillot, V., Davaillie, A., Besse, J., and Stock, J., 2003, Three distinct types of hotspots in the Earth's mantle: Earth and Planetary Science Letters, v. 205, p. 295-308.
Craig, H., and Lupton, J. E., 1981, Helium-3 and mantle volatiles in the ocean and the oceanic crust, *in* Emiliani, C., ed., The Sea, Volume 7: New York, Wiley, p. 391-428.
Craig, H., Lupton, J. E., Welhan, J. A., and Poreda, R., 1978, Helium isotope ratios in Yellowstone and Lassen Park volcanic gases: Geophys. Res. Lett., v. 5, no. 11, p. 897-900.
Cross, T. A., and Pilger, R. H., 1978, Constraints on absolute motion and plate interaction inferred from Cenozoic igneous activity in the western United States: American Journal of Science, v. 278, p. 865-902.
Davies, G. F., 1999, Dynamic Earth: Plates, Plumes and Mantle Convection, Cambridge, Cambridge University Press, 458+xi p.:
Dueker, K., Yuan, H., and Zurek, B., 2001, Thick-structured Proterozoic lithosphere of the Rocky Mountain region: GSA Today, v. 11, p. 4-9.
Dueker, K. G., and Sheehan, A. F., 1997, Mantle discontinuity structure from midpoint stacks of converted *P* to *S* waves across the Yellowstone hotspot track: Journal of Geophysical Research, v. 102, p. 8313-8327.

Eaton, G. P., Christiansen, R. L., Iyer, H. M., Pitt, A. M., Mabey, D. R., Blank, J. R. J., Zietz, I., and Gettings, M. E., 1975, Magma beneath Yellowstone National Park: Science, v. 188, p. 787-796.

Erslev, E. A., 1983, Pre-Beltian geology of the southern Madison Range, southwestern Montana.

Faccenna, C., Becker, T., Lallemand, S., Lagabrielle, Y., Funiciello, F., and Piromallo, C., 2010, Subduction-triggered magmatic pulses: A new class of plumes?: Earth and Planetary Science Letters, v. 299, p. 54-68.

Farnetani, C. G., and Richards, M. A., 1994, Numerical investigations of the mantle plume initiation model for flood basalt events: Journal of Geophysical Research, v. 99, p. 13813-13833.

Fee, D., and Dueker, K. G., 2004, Mantle transition zone topography and structure beneath the Yellowstone hotspot: Geophysical Research Letters, v. 31.

Ford, M. T., Grunder, A. L., and Duncan, R. A., 2012, Bimodal volcanism of the High Lava Plains and northwestern Basin and Range of Oregon: Distribution and tectonic implications of age-progressive rhyolites: Geochemistry Geophysics Geosystems, v. 14, no. 8.

Fouch, M. J., 2014, The Yellowstone Hotspot: Plume or Not?: Geology, v. 40, p. 479-480.

Foulger, G. R., 1988a, Hengill triple junction, SW Iceland; 1. Tectonic structure and the spatial and temporal distribution of local earthquakes: Journal of Geophysical Research, v. 93, no. B11, p. 13493-13506.

-, 1988b, Hengill triple junction, SW Iceland; 2. Anomalous earthquake focal mechanisms and implications for process within the geothermal reservoir and at accretionary plate boundaries: Journal of Geophysical Research, v. 93, p. 13,507-513,523.

-, 2010, Plates vs Plumes: A Geological Controversy, Wiley-Blackwell, Chichester, U.K., xii+328 p.:

Foulger, G. R., 2012, Are 'hot spots' hot spots?: Journal of Geodynamics, v. 58, p. 1-28.

Foulger, G. R., Jahn, C.-H., Seeber, G., Einarsson, P., Julian, B. R., and Heki, K., 1992, Post-rifting stress relaxation at the divergent plate boundary in Iceland: Nature, v. 358, no. 6386, p. 488-490.

Foulger, G. R., Miller, A. D., Julian, B. R., and Evans, J. R., 1995, Three-dimensional Vp and Vp/Vs structure of the Hengill triple junction and geothermal area, Iceland, and the repeatability of tomographic inversion: Geophysical Research Letters, v. 22, p. 1309-1312.

Foulger, G. R., Panza, G. F., Artemieva, I. M., Bastow, I. D., Cammarano, F., Evans, J. R., Hamilton, W. B., Julian, B. R., Lustrino, M., Thybo, H., and Yanovskaya, T. B., 2013, Caveats on tomographic images: Terra Nova, v. 25, p. 259-281.

Foulger, G. R., and Toomey, D. R., 1989, Structure and evolution of the Hengill-Grensdalur volcanic complex, Iceland; Geology, geophysics, and seismic tomography: Journal of Geophysical Research, v. 94, no. B12, p. 17511-17522.

Gao, S. S., and Liu, K. H., 2013, Imaging mantle discontinuities using multiply-reflected P-to-S conversions: Earth and Planetary Science Letters, v. 402, p. 99-106.

Geist, D., and Richards, M. A., 1993, Origin of the Columbia Plateau and Snake River Plain: deflection of the Yellowstone plume: Geology, v. 21, p. 789-792.

Ghosh, S., Ohtani, E., Litasov, K. D., Suzuki, A., Dobson, D., and Funakoshi, K., 2013, Effect of water in depleted mantle on post-spinel transition and implication for 660 km seismic discontinuity: Earth and Planetary Science Letters, v. 371–372, p. 103–111.

Gunasekera, R. C., Foulger, G. R., and Julian, B. R., 2003, Four dimensional tomography shows progressive pore-fluid depletion at The Geysers geothermal area, California: Journal of Geophysical Research, v. 108, no. B3, p. DOI: 10.1029/2001JB000638.
Hales, T. C., Abt, D. L., Humphreys, E. D., and Roering, J. J., 2005, Lithospheric instability origin for Columbia River flood basalts and Wallowa Mountains uplift in northeast Oregon: Nature, v. 438, p. 842-845.
Hanan, B. B., and Schilling, J.-G., 1997, The dynamic evolution of the Iceland mantle plume: the lead isotope perspective: Earth and Planetary Science Letters, v. 151, no. 1-2, p. 43-60.
Hart, S. R., Hauri, E. H., Oschmann, L. A., and Whitehead, J. A., 1992, Mantle plumes and entrainment: isotopic evidence: Science, v. 256, p. 517-520.
Heki, K., Foulger, G. R., Julian, B. R., and Jahn, C.-H., 1993, Plate kinematics near divergent boundaries: Geophysical implications of post-tectonic crustal deformation in NE Iceland detected using the Global Positioning System: Journal of Geophysical Research, v. 98, no. B8, p. 14279-14297.
Hill, D. P., 2006, Unrest in Long Valley Caldera, California: 1978-2004, *in* Troise, C., De Natale, G., and Kilburn, C. R. J., eds., Mechanisms of Activity and Unrest at Large Calderas, Volume Special Publication 269: London, Geological Society, p. 1-24.
Hoffman, P. F., 1989, Precambrian geology and tectonic history of North America, *in* Bally, A. W., and Palmer, A. R., eds., The Geology of North America – An overview, Volume A: Boulder, Colorado, Geological Society of America, p. 447-512.
Hofmann, A. W., 1997, Mantle geochemistry: the message from oceanic volcanism: Nature, v. 385, p. 219-229.
Hofmann, A. W., and White, W. M., 1982, Mantle plumes from ancient oceanic crust: Earth and Planetary Science Letters, v. 57, p. 421-436.
Hofton, M. A., and Foulger, G. R., 1996a, Post-rifting anelastic deformation around the spreading plate boundary, north Iceland, 1: Modeling of the 1987-1992 deformation field using a viscoelastic Earth structure: JGR, v. 101, p. 25,403 - 425,421.
-, 1996b, Post-rifting anelastic deformation around the spreading plate boundary, north Iceland, 2: Implications of the model derived from the 1987-1992 deformation field: Journal of Geophysical Research, v. 101, p. 25,423 - 425,436.
Hooper, P. R., Camp, V., Reidel, S., and Ross, M., 2007, The origin of the Columbia River flood basalt province: Plume versus nonplume models, *in* Foulger, G. R., and Jurdy, D. M., eds., Plates, Plumes, and Planetary Processes, Volume Special Paper 430: Denver, Colorado, Geological Society of America, p. 635-668.
Huang, S., Lee, C.-T. A., and Yin, Q.-Z., 2014, Missing lead and high $^{3}He/^{4}He$ in ancient sulfides associated with continental formation: Scientific Reports, v. 4, p. 1-6.
Humphreys, E. D., and Dueker, K. G., 1994, Physical state of the western U.S. upper mantle: Journal of Geophysical Research, v. 99, p. 9635–9650.
Humphreys, E. D., Dueker, K. G., Schutt, D. L., and Smith, R. B., 2000, Beneath Yellowstone; evaluating plume and nonplume models using teleseismic images of the upper mantle: GSA Today, v. 10, p. 1-7.
Hwang, Y. K., Ritsema, J., van Keken, P. E., Goes, S., and Styles, E., 2011, Wavefront healing renders deep plumes seismically invisible: Geophysical Journal International, v. 187, p. 273–277.
Iyer, H. M., Evans, J. R., Zandt, G., Stewart, R. M., Coakley, J. M., and Roloff, J. N., 1981a, A deep low-velocity body under the Yellowstone caldera, Wyoming: Delineation using teleseismic P-wave residuals and tectonic interpretation: Summary: Bulletin of the Geological Society of America, v. 92, p. 792-798.

Iyer, H. M., Oppenheimer, D. H., Hitchcock, T., Roloff, J. N., and Coakley, J. M., 1981b, Large teleseismic P-wave delays in The Geysers-Clear Lake geothermal area, *in* McLaughlin, R. J., and Donnelly-Nolan, J. M., eds., Research in The Geysers-Clear Lake Geothermal Area, Northern California, Volume 1141, p. 97-116.

James, D. E., Fouch, M. J., Carlson, R. W., and Roth, J. B., 2011, Slab fragmentation, edge flow and the origin of the Yellowstone hotspot track: Earth and Planetary Science Letters, v. 311, p. 124-135.

Karlstrom, K. E., Bowring, S. A., Chamberlain, K. R., Dueker, K. G., Eshete, T., Erslev, E. A., Farmer, G. L., Heizler, M., Humphreys, E. D., Johnson, R. A., Keller, G. R., Kelley, S. A., Levander, A., Magnani, M. B., Matzel, J. P., McCoy, A. M., Miller, K. C., Morozova, E. A., Pazzaglia, F. J., Prodehl, C., Rumpel, H.-M., Shaw, C. A., Sheehan, A. F., Shoshitaishvili, E., Smithson, S. B., Snelson, C. M., Stevens, L. M., Tyson, A. R., and Williams, M. L., 2002, Structure and evolution of the lithosphere beneath the Rocky Mountains: Initial results from the CD-ROM experiment: Geology, v. 12, p. 4-10.

Katsura, T., Yamada, H., Nishikawa, O., Song, M., Kubo, A., Shinmei, T., Yokoshi, S., Aizawa, Y., Yoshino, T., Walter, M. J., and Ito, E., 2004, Olivine-wadsleyite transition in the system $(Mg,Fe)_2SiO_4$: Journal of Geophysical Research, v. 109, no. B02209.

Keller, R. A., Fisk, M. R., and White, W. M., 2000, Isotopic evidence for Late Cretaceous plume-ridge interaction at the Hawaiian hotspot: Nature, v. 405, p. 673-676.

Kennedy, B. M., Lynch, M. A., Reynolds, J. H., and Smith, S. P., 1985, Intensive sampling of noble gases in fluids at Yellowstone: I. Early overview of the data: regional patterns.: Geochimica et Cosmochimica Acta, v. 49, p. 1251-1261.

Kunz, M. A., Covington, H. R., and Schorr, L. J., 1992, An overview of basaltic volcanism of the Eastern Snake River Plain, Idaho.

Lawrence, R. D., 1976, Strike-slip faulting terminates the Basin and Range Province in Oregon: Geological Society of America Bulletin, v. 87, p. 846-850.

Lemieux, S., Ross, G. M., and Cook, F. A., 2000, Crustal geometry and tectonic evolution of the Archean crystalline bsement beneath the southern Alberta Plains, from new seismic reflection and potential-field studies: Canadian Journal of Earth Science, v. 37, p. 1473-1491.

Liu, L., and Stegman, D. R., 2012, Origin of Columbia River flood basalt controlled by propagating rupture of the Farallon slab: Nature, v. 482, p. 386-389.

Long, M. D., Till, C. B., Druken, K. A., Carlson, R. W., Wagner, L. S., Fouch, M. J., James, D. E., Grove, R. L., Schmerr, N., and Kincaid, C., 2012, Mantle dynamics beneath the Pacific Northwest and the generation of voluminous back-arc volcanism: Geochemistry Geophysics Geosystems, v. 13, no. Q0AN01.

Love, J. D., 1956, Summary of geologic history of Teton County, Wyoming during Late Cretaceous, Tertiary, and Quaternary times, 11th Annual Field Conference, Volume Wyoming Geological Association Guidebook: Jackson Hole, p. 140-150.

Love, J. D., J. C. Reed, J., Christiansen, R. L., and Stacy, J. R., 1973, Geologic block diagram and tectonic history of the Teton region, U.S. Geological Survey Miscellaneous Geologic Investigations Map I-730.

Lowenstern, J. B., Evans, W. C., Bergfeld, D., and Hunt, A. G., 2014, Prodigious degassing of a billion years of accumulated radiogenic helium at Yellowstone: Nature, v. 206, p. 355-358.

Lustrino, M., and Anderson, D. L., 2015, The mantle isotopic printer, *in* Foulger, G. R., King, S. D., and Lustrino, M., eds., Geological Society of America and American

Geophysical Union, Volume this volume, Geological Society of America and American Geophysical Union.

Mabey, D. R., Zietz, I., Eaton, G. P., and Kleinkopf, M. D., 1978, Regional magnetic patterns in part of the Cordillera in the Western United States, *in* Smith, R. B., and Eaton, G. P., eds., Cenozoic tectonics and regional geophysics of the western Cordillera, Volume Geological Society of America Memoir 152, p. 93-106.

MacLeod, N. S., Walker, G. W., and McKee, E. H., Geothermal significance of eastward increase in age of upper Cenozoic rhyolitic domes in southeastern Oregon, *in* Proceedings Second United Nations Symposium on Development and Use of Geothermal Resources1976, p. 465-474.

McQuarrie, N., and Rodgers, D. W., 1998, Subsidence of a volcanic basin by flexure and lower crustal flow; The eastern Snake River Plain, Idaho: Tectonics, v. 17, p. 203-220.

Meibom, A., Anderson, D. L., Sleep, N. H., Frei, R., Chamberlain, C. P., Hren, M. T., and Wooden, J. L., 2003, Are high $^3He/^4He$ ratios in oceanic basalts an indicator of deep-mantle plume components?: Earth and Planetary Science Letters, v. 208, p. 197-204.

Meibom, A., Sleep, N. H., Zahnle, K., and Anderson, D. L., 2005, Models for noble gases in mantle geochemistry: Some observations and alternatives, *in* Foulger, G. R., Natland, J. H., Presnall, D. C., and Anderson, D. L., eds., Plates, Plumes, and Paradigms, Volume Special Paper 388: Boulder, CO, Geological Society of America, p. 347-364.

Miller, A. D., Julian, B. R., and Foulger, G. R., 1998, Three-dimensional seismic structure and moment tensors of non-double-couple earthquakes at the Hengill-Grensdalur volcanic complex, Iceland: GJI, v. 133, p. 309-325.

Mittelstaedt, E., Ito, G., and van Hunen, J., 2011, Repeat ridge jumps associated with plume-ridge interaction, melt transport, and ridge migration: Journal of Geophysical Research, v. 116, no. B01102.

Monastero, F. C., Katzenstein, A. M., Miller, J. S., Unruh, J. R., Adams, M. C., and Richards-Dinger, K., 2005, The Coso geothermal field: A nascent metamorphic core complex: Bulletin of the Geological Society of America, v. 117, p. 1534-1553.

Montelli, R., Nolet, G., Dahlen, F., and Masters, G., 2006, A catalogue of deep mantle plumes: new results from finite-frequency tomography: Geochemistry Geophysics Geosystems, v. 7, no. Q11007.

Montelli, R., Nolet, G., Dahlen, F. A., Masters, G., Engdahl, R. E., and Hung, S.-H., 2004a, Finite frequency tomography reveals a variety of plumes in the mantle: Science, v. 303, p. 338-343.

Montelli, R., Nolet, G., Masters, G., Dahlen, F., and Hung, S.-H., 2004b, Global P and PP traveltime tomography: rays versus waves: Geophysical Journal International, v. 158, p. 637–654.

Moreira, M., and Sarda, P., 2000, Noble gas constraints on degassing processes: Earth and Planetary Science Letters, v. 176, p. 375-386.

Morgan, W. J., 1971, Convection plumes in the lower mantle: Nature, v. 230, p. 42-43.

Morgan, W. J., 1972a, Deep mantle convection plumes and plate motions: Bulletin of the American Association of Petroleum Geologists, v. 56, p. 203-213.

Morgan, W. J., 1972b, Plate motions and deep mantle convection: Geological Society of America Bulletin, v. 132, p. 7-22.

Natland, J. H., 2003, Capture of mantle helium by growing olivine phenocrysts in picritic basalts from the Juan Fernandez Islands, SE Pacific: J. Pet., v. 44, p. 421-456.

O'Neill, J. M., and Lopez, D. A., 1985, Character and regional significance of Great Falls tectonic zone, east-central Idaho and west-central Montana: Am. Assoc. Petrol. Geol. Bull., v. 69, p. 437-447.

Obrebski, M., Allen, R. M., Xue, M., and Hung, S.-H., 2010, Slab-plume interaction beneath the Pacific Northwest: Geophysical Research Letters, v. 37, no. L14305.

Ozima, M., and Igarashi, G., 2000, The primordial noble gases in the Earth: a key constraint on Earth evolution models: Earth and Planetary Science Letters, v. 176, p. 219-232.

Parsons, T., Thompson, G. A., and Smith, R. P., 1998, More than one way to stretch: A tectonic model for extension along the plume track of the Yellowstone hotspot and adjacent Basin and Range Province: Tectonics, v. 17, p. 221-234.

Pavlis, G. L., Sigloch, K., Burdick, S., Fouch, M. J., and Vernon, F. L., 2012, Unraveling the geometry of the Farallon plate: Synthesis of three-dimensional imaging results from USArray: Tectonophysics, v. 532-535, p. 82-102.

Payne, S. J., R., M., and King, R. W., 2008, Strain rates and contemporary deformation in the Snake River Plain and surrounding Basin and Range from GPS and seismicity: Geology, v. 36, p. 647-650.

Pierce, K. L., and Morgan, L. A., 1992, The track of the Yellowstone hotspot: Volcanism, faulting, and uplift, *in* Link, P. K., Kuntz, M. A., and Platt, L. B., eds., Regional geology of eastern Idaho and western Wyoming, Volume 179, p. 1–53.

-, 2009, Is the track of the Yellowstone hotspot driven by a deep mantle plume? – Review of volcanism, faulting, and uplift in light of new data: Journal of Volcanology and Geothermal Research, v. 188, p. 1-25.

Pierce, K. L., Morgan, L. A., and Saltus, R. W., 2002, Yellowstone plume head: Postulated tectonic relations to the Vancouver slab, continental boundaries, and climate, in Bonnichsen, B., et al., eds., Tectonic and magmatic evolution of the Snake River Plain Volcanic Province: Idaho Geological Survey Bulletin, v. 30, p. 5-33.

Presnall, D. C., 1995, Phase diagrams of Earth-forming minerals, in mineral physics and crystallography: A handbook of physical constants, *in* Ahrens, T. J., ed., AGU Reference Shelf, Volume 2: Washington D.C., American Geophysical Union, p. 248-268.

Puskas, C. M., and Smith, R. B., 2009, Intraplate deformation and microplate tectonics of the Yellowstone hot spot and surrounding western U.S. interior: Journal of Geophysical Research, v. 114, no. B04410.

Puskas, C. M., Smith, R. B., Meertens, C. M., and Chang, W. L., 2007, Crustal deformation of the Yellowstone-Snake River Plain volcano-tectonic system: Campaign and continuous GPS observations, 1987-2004: Journal of Geophysical Research, v. 112, no. B03401.

Riley, P., Tikoff, B., and Hildreth, W., 2012, Transtensional deformation and structural control of contiguous but independent magmatic systems: Mono-Inyo Craters, Mammoth Mountain, and Long Valley Caldera, California: Geosphere, v. 8, p. 740-751.

Ritsema, J., and Allen, R. M., 2003, The elusive mantle plume: Earth and Planetary Science Letters, v. 207, p. 1-12.

Ritsema, J., van Heijst, H. J., and Woodhouse, J. H., 1999, Complex shear wave velocity structure imaged beneath Africa and Iceland: Science, v. 286, p. 1925-1928.

Rodgers, D. W., Chadwick, J. D., and Payne, S., 2005, Contemporary tectonic motion of the eastern Snake River Plain, Idaho: A global positioning system study, 1995-2004, Geological Society of America Abstract Programs, Volume 37.

Rodgers, D. W., Hackett, W. R., and Ore, H. T., 1990, Extension of the Yellowstone Plateau, eastern Snake River Plain, and Owyhee Plateau: Geology, v. 18, p. 1138-1141.

Rodgers, D. W., Ore, H. T., Bobo, R., McQuarrie, N., and Zentner, N., 2002, Extension and subsidence of the eastern Snake River Plain, *in* Bonnichsen, B., White, C., and

McCurry, M. O., eds., Tectonic and Magmatic Evolution of the Snake River Plain Volcanic Province, Volume 30, Idaho Geological Survey Bulletin, p. 121-160.
Schilling, J.-G., 1973, Iceland mantle plume: Geochemical study of Reykjanes ridge: Nature, v. 242, p. 565-571.
Schmandt, B., Dueker, K., Humphreys, E., and Hansen, S., 2012, Hot mantle upwelling across the 660 beneath Yellowstone: Earth and Planetary Science Letters, v. 331-332, p. 224-236.
Schmandt, B., and Humphreys, E., 2010, Complex subduction and small-scale convection revealed by body-wave tomography of the western United States upper mantle: Earth and Planetary Science Letters, v. 297, p. 435-445.
Shen, Y., Solomon, S. C., Bjarnason, I. T., Nolet, G., Morgan, W. J., Allen, R. M., Vogfjord, K., Jakobsdottir, S., Stefansson, R., Julian, B. R., and Foulger, G. R., 2002, Seismic evidence for a tilted mantle plume and north-south mantle flow beneath Iceland: Earth and Planetary Science Letters, v. 197, p. 261-272.
Sheth, H. C., 2007, Plume-related regional pre-volcanic uplift in the Deccan Traps: Absence of evidence, evidence of absence, *in* Foulger, G. R., and Jurdy, D. M., eds., Plates, Plumes, and Planetary Processes, Volume Special Paper 430: Boulder, CO, Geological Society of America, p. 785-813.
Silver, P. G., Behn, M. D., Kelley, K., Schmitz, M., and Savage, B., 2006, Understanding cratonic flood basalts: Earth and Planetary Science Letters, v. 245, p. 190-201.
Sleep, N. H., 1997, Lateral flow and ponding of starting plume material: JGR, v. 102, no. B5, p. 10,001-010,012.
Smith, R. L., and Luedke, R. G., 1984, Potentially active volcanic lineaments and loci in Western Conterminous United States, in Studies in Geophysics, Explosive volcanism: Inception, evolution, and hazards, Washington, D.C., National Academy Press, 47-66 p.:
Steinberger, B., Sutherland, R., and O'Connell, R. J., 2004, Prediction of Emperor-Hawaii seamount locations from a revised model of global plate motion and mantle flow: Nature, v. 430, p. 167-173.
Sun, D., and Helmberger, D., 2011, Upper-mantle structures beneath USArray derived from waveform complexity: Geophysical Journal International, v. 184, p. 416–438.
Takahahshi, E., Nakajima, K., and Wright, T. L., 1998, Origin of the Columbia River basalts: Melting model of a heterogeneous plume head: Earth and Planetary Science Letters, v. 162, no. 1-4, p. 63-80.
Thatcher, W., Foulger, G. R., Julian, B. R., Svarc, J., Quilty, E., and Bawden, G. W., 1999, Present-day deformation across the Basin and Range Province, Western United States: Science, v. 283, p. 1714-1718.
Thomas, M. D., Sharpton, V. L., and Grieve, R. A. F., 1987, Gravity patterns and Precambrian structure in the North America central plains: Geology, v. 15, p. 289-492.
Tian, Y., Sigloch, K., and Nolet, G., 2009, Multiple-frequency SH-wave tomography of the western US upper mantle: Geophysical Journal International, v. 178, p. 1384-1402.
Tian, Y., and Zhao, D. P., 2012, P-wave tomography of the western United States: Insight into the Yellowstone hotspot and the Juan de Fuca slab: Earth and Planetary Science Letters, v. 200-201, p. 72-84.
Vacher, P., Mocquet, A., and Sotin, C., 1998, Computation of seismic profiles from mineral physics: the importance of the non-olivine components for explaining the 660 km depth discontinuity: Physics of the Earth and Planetary Interiors, v. 106, p. 275-298.
Weaver, C. S., and Hill, D. P., 1978, Earthquake swarms and local crustal spreading along major strike−slip faults in California: Pure and Applied Geophysics, v. 117, p. 51−64.

Welhan, J. A., 1981, Carbon and hydrogen gases in hydrothermal system: The search for a mantle source [Ph.D. Ph.D.]: University of California, 216 p.
Wernicke, B., and Snow, J. K., 1998, Cenozoic tectonism in the central Basin and Range: Motion of the Sierran-Great Valley block: International Geology Review, v. 40, p. 403-410.
Wood, B. J., 1995, The effect of H_2O on the 410-kilometer seismic discontinuity: Science, v. 268, p. 74-76.
Xue, M., and Allen, R. M., 2010, Mantle structure beneath the western United States and its implications for convection processes: Journal of Geophysical Research, v. 115, no. B07303.
Yuan, H., and Dueker, K. G., 2005, Teleseismic P-wave tomogram of the Yellowstone plume: Geophysical Research Letters, v. 32, no. L07304.